ADDIS ABABA UNIVERSITY

ADDIS ABABA INSTITUTE OF TECHNOLOGY

SCHOOL OF CIVIL AND ENVIRONMENTAL ENGINEERING

APPLICATION OF MACHINE LEARNING METHODES FOR SHEAR CAPACITY OF RC BEAMS

A Thesis in Structural Engineering

By Birhane Gemeda Wakjira

Addis Ababa

December 2021

A Thesis

Submitted in Partial Fulfillment of the Requirements for the Degree of Master of Science

The undersigned have examined the thesis entitled '**Application of Machine Learning Methods for Shear Capacity of RC Beams**' presented by **Birhane Gemeda Wakjira**, a candidate for the degree of **Master of Science in Civil Engineering (Structures)** and hereby certify that it is worthy of acceptance.

Dr. Bedilu Habte		Feb 10/2022
Advisor	Signature	Date
Dr. Abriham Gebre		Feb 09/2022.
Internal Examiner	Signature	Date
Dr. Shifferaw Taye		20 December 2021
External Examiner	Signature	Date
Dr. Mebruk Mohammed		
Chairperson	Signature	Date

Mebruk Mohammed (Dr.-Ing.)
Dean, Sch... & Environmental Engineering

Director of Postgraduate Program
Addis Ababa University
Addis Ababa Institute of Technology

UNDERTAKING

I certify that research work titled “Application of Machine learning methods for shear capacity of RC beams” is my own work. The work has not been presented elsewhere for assessment. Where material has been used from other sources it has been properly acknowledged / referred.

Signature of Student

Name of Student: Birhane Gemeda Wakjira

ABSTRACT

Accurate determination of the capacity of reinforced concrete (RC) beams in shear remains a demanding problem due to its complex failure mechanism and the nonlinear relationship between different factors influencing the shear capacity. This research employs different types of single and ensemble machine learning (ML) based techniques; namely, decision tree, support vector machine, extremely randomized trees, gradient boosting, random forest, and extreme gradient boosting (xgBoost) to correctly predict the shear capacity of reinforced concrete beams. To this end, a dataset of experimental test results of RC beam with and without stirrups comprised of various beam geometry, concrete strength, reinforcing steel strength, longitudinal and shear reinforcement ratios, and shear span-to-effective depth ratio is used to develop the models.

The proposed models were calibrated for different values of hyperparameters to achieve optimized ML models. The results of the analysis evidenced that the xgBoost model can be effectively utilized to predict the shear capacity of RC beams. The comparison of the predictions of the proposed and existing models evidenced that the efficiency of the proposed model is superior to the existing models and guidelines in terms of accuracy, safety, and economic aspects with significantly lowest bias and variability.

A solid correlation exists between the shear capacities predicted using the proposed model and the corresponding experimental values as evidenced by the value of R^2 ($R^2 = 0.99$) for RC beams without stirrup and ($R^2 = 0.995$) for RC beams with stirrup.

The proposed xgBoost model is deployed into a user-friendly web-based application to facilitate a quick and accurate prediction of capacity of RC beams in shear. The web-based application can be used by both practitioners and researchers to accurately predict the shear capacity of beams.

Keywords

Shear Capacity Prediction; RC Beams; Machine Learning

ACKNOWLEDGMENTS

First and foremost, praises and thanks to the Almighty God, for His blessings throughout my research work to complete the research successfully.

I would like to express my deep sincere gratitude to my thesis advisor Dr. Bedilu Habte for his guidance and support

I am extremely grateful to my brother Dr. Tadesse Gemeda for his support and guidance. He has taught me the methodology to carry out the research and to present the research works as clearly as possible.

I am very much thankful to my mother for her love, prayers, caring and sacrifices for educating me. Also I express my thanks to my husband for his support to complete this research work.

TABLE OF CONTENTS

LIST OF TABLES

LIST OF FIGURES

CHAPTER 1 INTRODUCTION

1.1 Background

Shear failure is sudden and often catastrophic as it occurs without warning. On the contrary, flexural failure involves the yielding of reinforcement bars which is ductile as it provides enough warning. Thus, reinforced concrete (RC) beams should be designed with adequate shear capacity in order to avoid such catastrophic and sudden shear failure and assure ductile flexural failure. It is crucial to understand the shear behavior of RC beams for a safe, economical, accurate design of the beams. Despite the various research efforts, fully assessing the shear behavior of RC beams remains a challenging task when compared to assessing its flexural behavior that can be predicted with an acceptable accuracy [1,2]. This challenge lies in a complicated failure mechanism associated with shear-critical RC beams. Most design codes and guidelines including ACI 318 [3] and Eurocode 2 [4] for the shear strength of RC elements are empirically derived using a limited number of important factors. Hence, most of the available models results in unsafe and/or uneconomical design. As a result, a more rigorous prediction model is required for better understanding and safe design of reinforced concrete beams.

Machine learning (ML) has recently gained immense attention owing to its ability to effectively determine the relationship between the input features and the response (dependent) variable (s) in a complex system. It is considered as a powerful technique to solve different civil engineering problems [5–15]. This is attributed to their ability to estimate the relationship between the factors and the response parameter (s) [16]. In contrast to the case of most empirical models, ML techniques does not require the prior

assumption or knowledge of the underlying mathematical and physical models [16]. Some of the applications of ML techniques reported in the literature include the prediction of mechanical properties of concrete [6,8–10], load capacity and failure modes of RC columns and walls [11,17,18], and seismic damage assessment of RC buildings and bridges [19–21]. Artificial neural network (ANN) is among the most popular ML techniques [9]. It has been successfully employed for different structural engineering studies; some of which include the prediction of mechanical properties of concrete [6,8–10], damage assessment of bridges [22–24] and buildings [25], ultimate deformation capacity of RC columns [11], shear strength of circular RC columns [26], and compressive strength [13–15] and the stress-strain relationship [12] of concrete confined with FRP. A review of the application of different artificial intelligent techniques in the field of civil engineering is conducted by [5]. Support vector machine (SVM) is another powerful ML technique that has been applied to structural engineering problems [27–29]. Solhmirzaei et al. [29] used three different ML techniques, namely, SVM, k-nearest neighbor (kN), and ANN to classify the failure modes of Ultra High Performance Concrete (UHPC) beams. The results showed that ANN outperformed the other two methods in predicting the failure modes of UHPC beams with an overall accuracy of 89%. In this study, several ML techniques have been explored to propose the best predictive model for shear capacity of beams. Ensemble models are another type of emerging ML technique with high performance compared to other techniques. These algorithms combine two or more learners known as base learners (e.g. kernel regression, support vector machine, and decision tree) to enhance the efficiency, robustness, and stability of the base learners [30]. The basic idea behind the ensemble model is to combine multiple base learners in computing the final response rather than relying on an individual model. Ensemble

learners can be formed in sequential or parallel styles with the aim to exploit the dependence and independence between the base models, respectively. Bagging (short for **B**ootstrap **Agg**regating) [31] is one of the ensemble models in which multiple base learners are independently trained in parallel using different bootstrap sample. Each bootstrap training dataset contains an average of 63.2% of the original training set. The final prediction is then taken as the mean of the predictions from the base learners [31]. As a result a better prediction with reduced variance is obtained [31]. Random forest (RF) is a popular example of bagging ensemble learners. In RF homogeneous base learners, particularly, decision trees are used. An ensemble model can also be formed from multiple base learners of different types or heterogeneous base learners [30]. Stacking ensemble is one of the heterogeneous ensemble models in which different types of base learners are combined via a meta-model with the objective of enhancing the accuracy of the individual model [32,33].

In the previous study, different researchers have attempted to examine the efficacy of ML models to estimate the capacity of RC beams in shear [34–39]. Sanad and Saka [34] studied the application of ANN in predicting the capacity of deep RC beams in shear using the test results of only 111 RC beams considering 10 input variables. The results of the ANN-based model were compared against that of the ACI equation. The authors concluded that the shear capacity predictions from the ACI code equations are very conservative and thus uneconomical. The proposed ANN model outperformed the ACI equation in predicting the capacity of the beams in shear. However, it is worth mentioning here that a small number of datasets used to train ML algorithms will lead to overfitting and a false sense of high predictive performance. As per Friedman et al. [40], a sufficient training and testing

dataset should be at least 10 times the number of independent parameters. Chou et al. used support vector regression (SVR) for the prediction of the shear strength of RC deep beams based on a larger experimental data of 214 RC deep beams.

Cladera and Mari [35] investigated the application of ANN to predict the shear capacity of RC beams without stirrups based on the dataset of 177 experiments on RC beams. Five parameters; namely, effective beam depth, longitudinal reinforcement ratio, width of the beam, concrete compressive strength, and aspect ratio were considered as input parameters. The authors concluded that ANN can be applied to predict the shear capacity of RC beams without stirrups. In another study, the same authors applied ANN to predict the shear capacity of RC beams reinforced with stirrups based on the test results of 123 RC beams with stirrups.

Chou et al. [38] used different ML algorithms to estimate the shear strength of RC beams using the experimental dataset of RC beams compiled by Collins et al. [41] and Zhang et al. [42]. For RC beams reinforced without stirrups, the dataset comprises 1849 RC beam test results. However, the database used for RC beams with stirrups comprised only 194 test results of RC beams. In this study, different single models including multi-layer perceptron ANN, decision tree, support vector regression, linear regression, ensemble methods (voting, bagging, stacking), and hybrid ML models are used.

Despite the investigation of the application of ML techniques to predict the capacity of RC beams in shear, all the above studies generally failed to propose a user-friendly and practical shear design approach based on the results of the trained ML models. As it is well understood, ML algorithms are generally black-boxes and as such cannot be reproduced

by others. Thus, practical implementation and simplification of the ML-based models are essential. Moreover, most of the models are developed using a limited number of experimental datasets, which limits the generalization of the developed models.

In lieu of the above-mentioned limitations, the current study investigated the application of several ML models (both single and ensemble models) to propose the best predictive model based on a large database of slender and deep RC beams with/without stirrups. Moreover, the best model among the developed models is deployed into a user-friendly web-based application, which can be used by practitioners and researchers in the field of civil engineering to accurately determine the capacity of RC beams in shear. The developed web-based application facilitates a rapid and accurate prediction of the capacity of RC beams in shear.

1.2 Research objectives

This is a pioneer research work leveraging the power of different machine learning models to produce accurate and robust model for shear design of reinforced concrete (RC) beams. Machine learning models generally exhibit higher prediction capacity compared to statistical and empirical models; however, the accuracy of machine learning models can drastically vary from one type of problem to other. One of the reasons for the variation in the accuracy of the ML models with the problem type is attributed to the complex relationship of input and output. In this context, among different ML models, ensemble learners combine different base learners to produce a powerful model. Thus, this research is aimed to produce a robust ensemble machine learning model to accurately estimate the capacity of RC beams in shear considering key design factors that influence their shear

capacity. Moreover, a web-based application is developed using the best ML model. The developed web-based application can be easily utilized by practitioners or researchers in the field of Civil Engineering to accurately determine the capacity of RC beams in shear.

1.2.1 General objective

The main objectives of the current research are listed below.

- Develop a novel ML-based model for estimating the shear capacity of RC beams with/without stirrups.
- Compare the prediction accuracy of the proposed ensemble model with other machine learning models.
- Comparative investigation of the proposed model and existing shear design models and code equations.

1.2.2 Specific objective

- Collect a large database of RC beams experiments and preprocess the database.
- Identify the main factors that influence the shear capacity of RC beams based on a thorough literature review.
- Develop different ML models for predicting the capacity of RC beams in shear and select the best predictive model using different statistical performance indices.
- Compare the predictive capability of the proposed model with that of the existing models.
- Develop a simple and efficient web-based application, which can be used by practitioners and researchers in the field of civil engineering without the need of the knowledge of machine learning algorithms.

1.3 Scope

The scope of this thesis is to propose novel machine learning-based shear design models for RC beams with/without stirrups. Various ML-based are developed in order to propose the best shear capacity predictive models. Finally, the predictive performance of the proposed model is compared with that of the existing models.

1.4 Research Significance

There are different approaches and guidelines to determine the shear capacity of RC beams. Numerical, analytical, and mechanical models are widely-used models. All these models are based on assumptions hence fail short of producing accurate predictions. Besides, there are large discrepancies and uncertainty in the existing shear design models. One of such discrepancies is related to the selection of important factors in determining the shear capacity of RC beams. Furthermore, the existing empirical models are generally based on a simple truss analogy without considering the interaction between different factors and the variation of the shear crack angle. In contrast, a machine learning model learns the relationship between the input features and the response variable from data without prior assumption or knowledge of the underlying mathematical and physical models. In nature, machine learning models work better on large data to solve classification and regression problems. Therefore, this study is aimed to propose an accurate and reliable shear design model using different ML techniques considering all important parameters. To this end, a large database of experiments on RC beams was collected. The collected data comprised various beam geometries, material strengths for both concrete and steel, longitudinal and transverse reinforcement ratios, and shear span-

to-effective depth ratios. The performance of the ML model is greatly influenced by the value of its hyperparameters, which are parameters that control the learning process of a given ML model. The values of the hyperparameters for each ML model are tuned to obtain the best model. Finally, the prediction performance of the proposed ML models is compared with that of the existing models and code equations. A comparative investigation of the proposed and existing models revealed the superior prediction capability of the proposed model in terms of accuracy, safety, and economical aspects. Hence, this research is significant in assessing the best model in determining the shear capacity of RC beam and propose a robust predictive model.

1.5 Layout of work

Chapter 1 presents the background information of the study, objective, significance, scope, and methodology of the study. Chapter 2 presents a literature review on the shear strength of RC beam focused on parameters influencing the shear strength of RC beam and existing shear design models and code equations. Chapter 3 presents the experimental database used in this study. Different machine learning techniques are introduced in Chapter 4. Moreover, Chapter 4 discusses different single and ensemble ML models. Six ML models (two single models and four ensemble models) are analyzed in this chapter. Chapter 5 describes the results from the ML model and comparative study with existing models and code equations. The performance of each model is evaluated using different performance indices. Chapter 6 discuss the conclusion from this study and recommendations for future research.

1.6 Methodology

The following procedures will be followed in this research work.

- **Construction of database:** an extensive database of experimental results of deep and slender RC beams with/without stirrups critical in shear will be compiled form the literature.
- **Identification of input parameters**: this is a critical stage in the development of ML models. The input variables that affect the capacity of RC beams will be identified based on a thorough literature survey.
- **Data processing**: the third step in the development of ML models is the preprocessing of the collected database, which includes but is not limited to the identification of outliers and normalization of the database.
- **Hyperparameter tuning**: the performance of ML models depends on the values of hyperparameters, which are parameters that control the learning process of a given ML model. The hyperparameters for each model will be tuned carefully to achieve superior prediction accuracy. In order to select the best predictive model, different performance indices will be used.
- **Model training, validation, and testing**: the database will be randomly split into test and train datasets. The training database will be used for the model training and development, while the testing dataset will be used to finally appraise the performance of the ML models.
- **Comparative study**: the efficacy of the proposed models will be finally compared with that of the existing models and code equations including ACI 318 and Eurocode.

CHAPTER 2 LITERATURE REVIEW

2.1 Shear strength of RC beam

The formation of diagonal tension crack occurring at an angle with respect to the beam axis causes the shear failures. Shear failure is sudden and occurs without prior warning, thus it is a brittle failure, unlike flexural failure. Hence, it is vital to make sure that the shear supply is greater than the shear demand in order to avoid such undesirable shear failure. The primary goal of shear design is to prevent such failure and ensure flexural failure. However, shear failure involves a complex failure mechanism, and as such difficult to develop simple models like that used to characterize flexural behavior, where the assumption of plane sections remain plane is valid. Several studies have been conducted to propose shear strength models based on the principles of mechanics. Shear behavior is the sum of various mechanisms, thus difficult to establish a mechanics-based shear design model. The free-body diagram in **Figure 2.1** shows the internal forces in RC beam after the formation of diagonal shear crack.

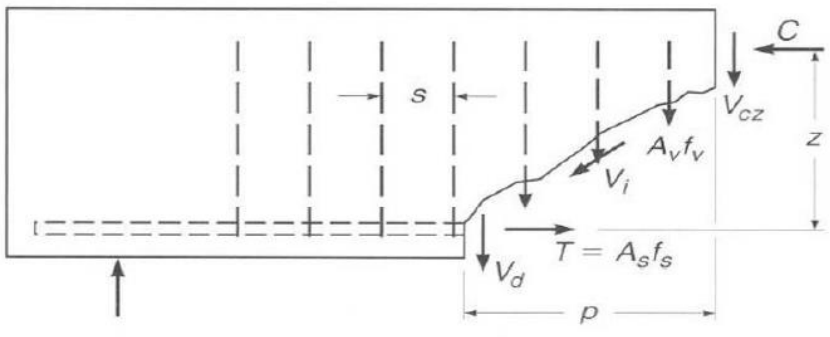

Figure 2.1: Internal forces along diagonal shear crack [43].

In the above figure, C denotes uncracked compressive force in uncracked concrete, V_{cz} is the shear in the compression zone, V_s is the shear capacity provided by transverse reinforcement, V_i is the shear capacity provided by the aggregate interlock, T is the tension force in longitudinal reinforcement bars, and V_d is the dowel action of longitudinal reinforcement bars.

The shear force in RC beams is resisted by different mechanisms including transverse reinforcement (stirrups), aggregate interlock, uncracked concrete, and dowel action of the flexural bars [44,45]. For instance, **Figure 2.2** illustrates the relative contributions of different mechanisms to the capacity of RC beams without stirrups at a cracked section. As can be seen in this figure, concrete aggregate interlock provides the highest shear capacity compared to dowel action of flexural reinforcement and uncracked concrete contribution in the compression zone. Various factors influence the shear capacity of RC beams. The following section briefly discusses the influence of different key variables on the capacity of RC beams in shear.

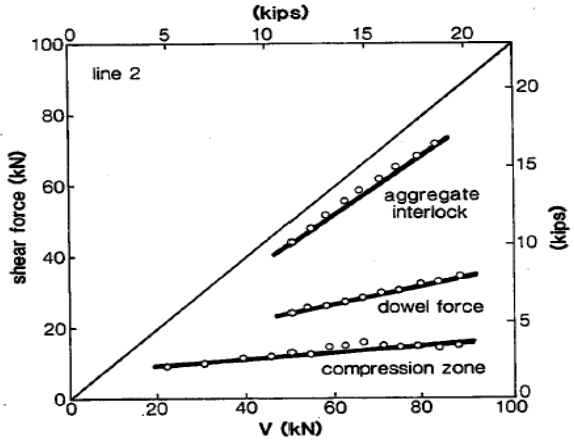

Figure 2.2: Components of shear resistance at cracked concreate section for RC beams without stirrup [46]**.**

2.2 Parameters influencing shear strength of RC beam

The shear capacity of RC beams is influenced by different factors: concrete compressive strength, yield strength and reinforcement ratio of stirrups, cross-sectional depth of the beam, a/d ratio, and longitudinal reinforcement ratio, as will be discussed below.

2.2.1 Concrete compressive strength

Previous studies reported an improvement in the shear strength of RC beams with increasing concrete compressive strength (f_c). However, there is inconsistency in the formulations for the shear strength provided by concrete. For instance, according to ACI 318-14 [47], the concrete contribution to shear capacity has been assumed to be $2\sqrt{f_c'}\ bd$. However, in Eurocode 2 [4], the shear strength is correlated with the cubic root of f_c', $V \propto \sqrt[3]{f_c'}$. Shear forces are transmitted through concrete cracks by virtue of roughness of the concrete interfaces.

2.2.2 Transverse shear reinforcement

As it is well understood, the provision of transverse reinforcement (stirrups) increases the shear strength of RC beams which in turn increases their ductility. In addition to providing additional shear strength, stirrups are used to hold the main reinforcements and link together the flexural compression and tension sides of a member and ensure that the two sides act as a unit. Breakdown of those linkages may cause shear failure. Besides, shear reinforcement limits the development of inclined cracks and prevents the cracks from widening. The strain in shear reinforcement prior to the onset of crack is equal to that in concrete. However, with the formation of the inclined cracks shear reinforcement contributes substantially to shear resistance as diagonal tension cracks form at very small strains. The contribution of stirrups to the capacity of RC beams in shear depends on the diameter and spacing of stirrups.

2.2.3 Depth

Increasing the effective depth of RC beams intuitively increases the shear capacity of the beams. In most of the models and code equations, the shear capacity of RC beams is directly proportional to the effective depth of the beam. The average shear strength at the failure of beams is reduced by an increase in the beam depth.

2.2.4 Longitudinal reinforcement ratio

The longitudinal reinforcement provides shear resistance through the dowel action. In addition to providing an enhanced dowel action, the presence of increased longitudinal reinforcement controls the propagation of flexural cracks and leads to an increase in the neutral axis depth, which in turn increases the depth of uncracked concrete in compression. The increase in the depth of uncracked concrete in compression, in turn, enhances the shear

capacity of the beam. Thus, an increase in the longitudinal reinforcement ratio enhances the shear strength of the beam owing to an increase in dowel action [48–50]. However, there is a discrepancy in international codes and standards for the shear design of RC beams in accounting for the shear strength provided by longitudinal reinforcement. For instance, in Eurocode2 [4], the shear strength of RC beams has a direct relation with the cubic root of the longitudinal reinforcement ratio (ρ_{sx}). However, this effect has not been considered in ACI 318 [3].

2.2.5 Shear span-to-depth ratio

The shear span-to-depth (a/d) ratio is another important factor that influences the shear capacity of RC beam. However, it has a distinct effect on different shear resisting mechanisms. The concrete contribution to the shear capacity decreases as a/d ratio increases [51]. However, the shear strength provided by transverse reinforcement increases with an increase in a/d ratio [51]. In addition, shear resistance provided by first diagonal crack is significantly larger than shear resistance provided by concrete when the shear span-to-depth ratio is large but much smaller than shear resistance provided by concrete when a/d ratio is small. Generally, an increase in a/d ratio cause reduction of ultimate shear capacity of RC beams [51].

2.3 Existing Shear Design Model and Guideline

There exist different standards and models for shear capacity determination of RC beams. Collins et al. [52] provided a review on the shear models proposed in the early 20th century (1948 to 2008). In a traditional truss analogy of Ritter and Morsch, the shear stress was assumed to be resisted by stirrups and diagonal compressive concrete struts inclined at 45°

to the beam height [53]. According to this model, the ultimate shear capacity of the beam corresponds to the yielding of the stirrups, while neglecting the tensile stress in a cracked concrete and thus gives a conservative prediction [54]. Moreover, the model ignores the shear resisted by uncracked concrete section, aggregate interlock along the cracks, and dowel action of the longitudinal reinforcement [53]. The truss model has provided a basis for different codes of practice including ACI 318-14 [55] and Eurocode-2 (2004) [4] standards. ACI 318-14 standard assumes a constant strut angle of 45° while considering the contribution of the concrete in the tension. On the other hand, Eurocode-2 (2004) is based on a variable angle truss model but ignores concrete contribution to the shear strength for beams reinforced with ITSR. The most widely used models and code equations are summarized in Table 2.1 and discussed in the following subsections.

Table 2.1: Shear capacity of RC beams according to different models

Reference	Formulation
Eurocode 2 [4]	• Members without internal transverse reinforcement $V_n = V_{Rd,c} = C_{Rd,c}k(100\rho_{sx}f_c')^{1/3}b_w d$ (f_c' is in MPa) $k = 1 + \sqrt{\frac{200}{d}} \leq 2.0$ (d in mm) $\rho_{sx} \leq 0.02$ $C_{Rd,c} = \frac{0.18}{\gamma_c}, \quad \gamma_c = 1.5$ • Members with internal transverse reinforcement $V_n = V_{Rd,s} = \rho_{sv}f_{svd}b_w Z\cot\theta \leq \alpha_{cw}b_w Z\nu_1 f_{cd}/(\cot\theta + \tan\theta)$ $f_{svd} = 0.8f_{sv}$ $1 \leq \cot\theta \leq 2.5$ $Z = 0.9d$ $\alpha_{cw} = 1$, for non-prestressed beam

	$v_1 = \begin{cases} 0.6 & \text{for } f_c' \leq 60 \text{ MPa} \\ 0.9 - \frac{f_c'}{200} > 0.5 & \text{for } f_c' \geq 60 \text{ MPa} \end{cases}$
AASHTO-LRFD [56]	$V_n = \beta\lambda\sqrt{f_c'} + \rho_{sv} f_{sv} b_w d \cot\theta$ (f_c' is in MPa) where, $\beta = \begin{cases} \frac{0.4}{1+750\varepsilon_x}, & \text{for section with minimum amount of ISR} \\ \frac{0.4}{1+750\varepsilon_x}\frac{1300}{1000+S_{xe}}, & \text{esle} \end{cases}$ $\theta = 29 + 3500\varepsilon_{sx}$
ACI 318 [47]	$V_n = V_c + V_s$ $V_c = \left(\frac{\sqrt{f_c}}{6}\right) b_w d, \quad f_c < 70$ MPa $V_s = \frac{A_{sw}}{S} d f_{yt}$
JSCE 2007 [57]	$V_c = 0.9\beta_d\beta_p\beta_0 f_c^{1/3} b_w d$ where, $\beta_d = \left(\frac{100}{d}\right)^{1/4} \leq 1.5$ $\beta_p = (100\rho)^{1/3} \leq 1.5$ $\beta_0 = 0.75 + [1.4/(a/d)]$ $V_s = \frac{A_{sw}}{S} f_{yw}(j_t \cos\theta)$
CSA A23.3-94 (simplified method) [58]	$V_n = V_c + V_s$ $V_c = 0.2\sqrt{f_c'} b_w d \;\; when, A_{sw} \geq \frac{0.06\sqrt{f_c'} b_w s}{f_y} \;\; or\ d \leq 300\ mm$ $or\ V_c = \frac{260}{1000+d}\sqrt{f_c'} b_w d$ $when, A_{sw} \leq \frac{0.06\sqrt{f_c'} b_w s}{f_y} \;\; or\ d \geq 300\ mm$ $V_s = \frac{A_{sw}}{S} d f_{yt}$ where, $V_s \leq 0.8\sqrt{f_c'} b_w d$

2.3.1 ACI 318 [47]

According to ACI 318 [47], the shear capacity of RC beam is evaluated as a simple superposition of the capacity provided by concrete (V_c) and stirrups (V_s). **Figure 2.3** depicts the shear contributions provided by stirrups and concrete. Thus, in ACI 318, the nominal shear capacity (V_n) is determined as:

$$V_n = V_c + V_s \tag{1}$$

$$V_c = \left(\frac{\sqrt{f_c}}{6}\right) b_w d, \quad f_c < 70 \text{ MPa} \tag{2}$$

$$V_s = \frac{A_{sw}}{S} d f_{yt} \tag{3}$$

where,

$V_c =$ Shear capacity provided by concrete

$V_s =$Shear capacity provided by transverse reinforcement

$f_{yt} =$ Yield strength of stirrups

$b_w =$ Width of the web

$S =$ Spacing of the stirrups

$d =$ Effective depth of the beam section

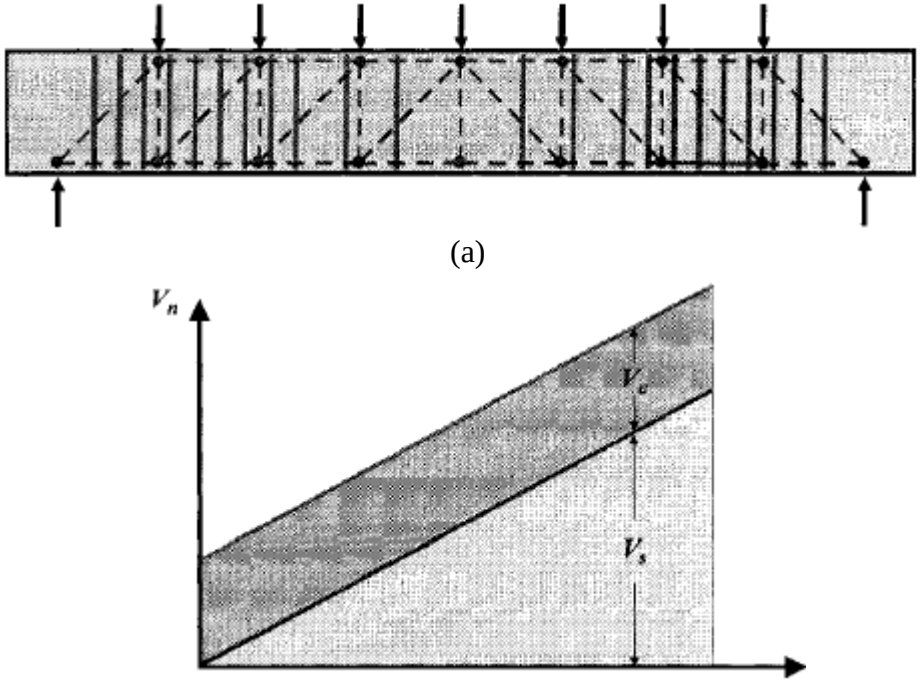

Figure 2.3: Concrete and stirrups shear resisting mechanisms (a) and graphical illustration of their contribution (b) [59]**.**

2.3.2 Eurocode (EC2) [4]

According to Eurocode (EC2) [4], different models are used to determine the capacity of RC beams with and without internal transverse reinforcement, as discussed below.

2.3.2.1 Members without internal transverse reinforcement

For beams without stirrups, the shear capacity is given by [4]:

$$V_n = V_{Rd,c} = C_{Rd,ck}\,(100\rho_{sx}f_c')^{1/3}b_w d \tag{4}$$

$$k = 1 + \sqrt{\frac{200}{d}} \leq 2.0 \tag{5}$$

$$\rho_{sx} \leq 0.02$$

$$C_{Rd,c} = \frac{0.18}{\gamma_c}, \quad \gamma_c = 1.5 \tag{6}$$

where ρ_{sx} is the longitudinal reinforcement ratio.

2.3.2.2 Members with internal transverse reinforcement

For beams internally reinforced with stirrups, the shear capacity is given by [4]:

$$V_n = V_{Rd,c} = \rho_{st} f_{std} b_w Z cos\theta \leq \alpha_{cw} b_w Z v_1 f_{cd} / (cos\theta + tan\theta) \tag{7}$$

$$f_{std} = 0.8 f_{yt} \tag{8}$$

$$Z = 0.9d \tag{9}$$

$$1 \leq cos\theta \leq 2.5 \tag{10}$$

$$v_1 = 0.6 \text{ for } f_c' \leq 60MPa$$
$$v_1 = 0.9 - \frac{f_c'}{200} > 0.5 \text{ for } f_c' \geq 60MPa \tag{11}$$

where,

θ = shear crack angle relative to the longitudinal axis of the beam, and

$\alpha_{cw} = 1$, for non-prestressed beam.

2.3.3 JSCE (2007) [57]

The Japanese JSCE code (2007) [57] considers the effect of effective depth of member, the reinforcement ratio of longitudinal bars, and the concrete compressive strength in its model to estimate the concrete contribution to shear strength of RC members, as follows:

$$V_c = \beta_d \beta_p \beta_n f_{vcd} b_w d / \gamma_b \tag{12}$$

$$f_{vcd} = 0.20\sqrt[3]{f'_{cd}} \leq 0.72 \text{ (MPa)} \quad (13)$$

$$\beta_d = \left(\frac{100}{d}\right)^{1/4} \leq 1.5, \qquad (d \text{ in mm}) \quad (14)$$

$$\beta_p = (100\rho_{st})^{1/3} \quad (15)$$

$$0 \leq \beta_n = 1 + \frac{2M_0}{M_{ud}} \leq 2.0, for\ N'_d \geq 0 \quad (16)$$

where,

β_d = Depth factor,

N'_d = Design axial force,

β_d = Factor accounting for the effect of ρ_{sx},

β_n = Factor accounting for the effect of a/d ratio,

M_0 = Flexural moment required to balance the stress due to axial load at the extreme tension fiber,

M_{ud} = Pure flexural capacity neglecting the effect of axial force, and

γ_b = Member factors, generally taken as 1.30.

For members without axial load the value of β_n is unity.

2.3.4 CSA A23.3-94 (Simplified Method) [58]

The simplified method of Canadian Standard [58] is based on the 45-degree truss model. The shear capacity of RC beam is evaluated as a simple superposition of the capacity provided by stirrups and concrete, as follows:

$$V_c = 0.2\sqrt{f_c'}b_w d \;\; when \quad A_{sw} \geq \frac{0.06\sqrt{f_c'}b_w s}{f_y} \;\; or\; d \leq 300\; mm$$

$$V_c = \frac{260}{1000 + d}\sqrt{f_c'}b_w d \; A_{sw} \leq \frac{0.06\sqrt{f_c'}b_w s}{f_y} \;\; or\; d \geq 300\; mm \tag{17}$$

$$V_s = \frac{A_{sw}}{S} d f_{yt} \leq 0.8\sqrt{f_c'}b_w d \tag{18}$$

2.3.5 Modified compression field theory

The modified compression field theory (MCFT) [60] used the principles of equilibrium, compatibility, and constitutive relationship of the cracked concrete section to develop a shear model. Unlike the traditional truss-based models (e.g. ACI 318 [47]), the MCFT accounts for the contribution of the concrete tensile stresses of a cracked section. Moreover, a variable angle of diagonal struts was considered compared to the fixed value of 45° strut angle. The principles of compatibility, equilibrium and constitutive relationship of cracked concrete section of MCFT are shown in the figure below.

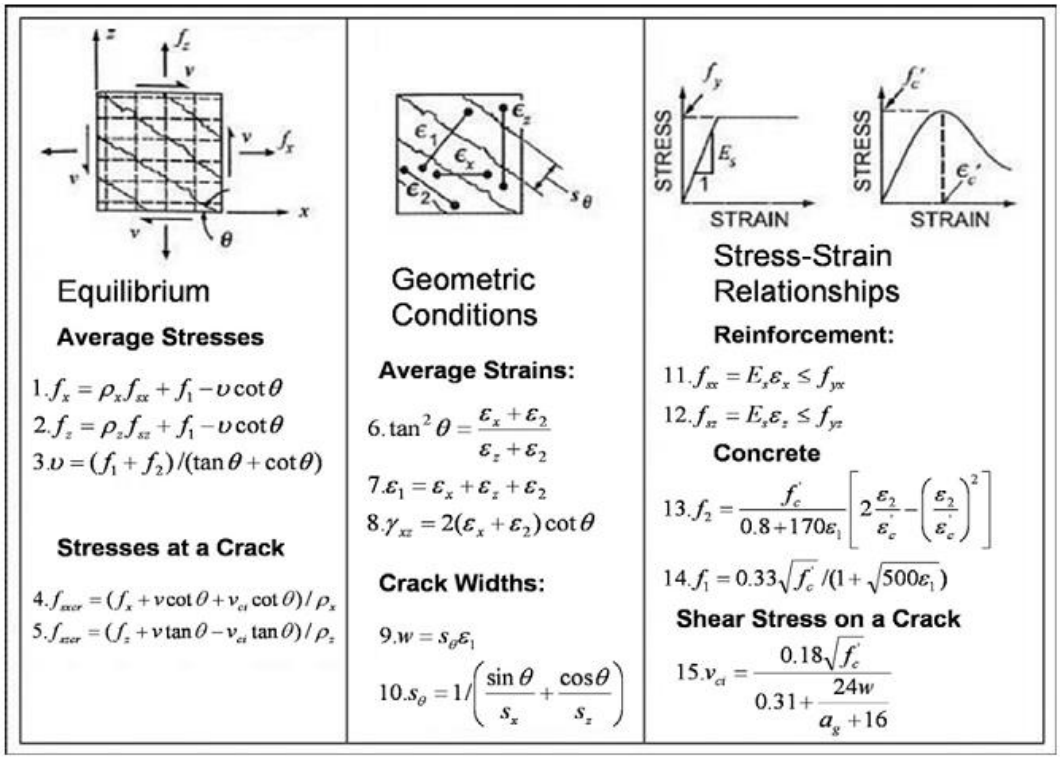

Figure 2.4: MCFT equations [46]

The MCFT entails solving a large number of equations iteratively [61,62]. To ease this procedure, Collins et al. [61] proposed a general method of shear design based on the MCFT where the shear capacity is determined as a function of tensile stress factor (β) and inclination of the principal compressive stress (θ). The authors provided a table for approximating the values of β and θ, for members with as well as without stirrups, for a limited range of longitudinal strain values ($\varepsilon_{sx} \le 0.2\%$). On the other hand, a simplified compression field theory (SCFT) was developed by Bentz et al. [62] in which the values of β and θ are determined as a function of the longitudinal tensile strain (ε_x) and crack spacing (S_{xe}). In the SCFT, simple expressions for β and θ are used, reducing the required number of parameters and iterations, while predicting the shear capacity of the concrete beam almost as accurately as the MCFT.

$$\beta = \frac{0.4}{1 + 1500\varepsilon_x}\frac{1300}{100 + s_{xe}} \tag{19}$$

$$S_{xe} = \frac{1}{\frac{\sin\theta}{s_{mx}} + \frac{\cos\theta}{s_{my}}} \tag{20}$$

For beams not reinforced with stirrup the crack spacing is given by as follows as per.

$$S_{xe} = \frac{35S_x}{a_g + 16} \geq 0.85S_x \tag{21}$$

$$\varepsilon_x = \frac{v\cot\theta - \beta\sqrt{f_c'}\tan\theta}{E_s\rho_{sx}} \tag{22}$$

$$\theta = (29 + 7000\varepsilon_x) \times \left(0.88 + \frac{S_{xe}}{2500}\right) \leq 75° \tag{23}$$

$$v = \beta\sqrt{f_c'} + \rho_{sy}f_{sy}\cot\theta \tag{24}$$

$f_{sx} = \varepsilon_x E_s \leq f_{yx}$

Thus, the shear capacity of RC beam is determined by, $V = vb_wd$

where,

s_{mx}= Average spacing perpendicular to the x-reinforcement (stirrups spacing)

s_{my}= Average crack spacing perpendicular to y-reinforcement (effective depth of the beam)

CHAPTER 3 EXPERIMENTAL DATABASE

This chapter presents the experimental database of shear critical RC beams (with and without stirrups). Data curation, which involves collection of relevant experimental results, data preprocessing, and identification of input and output variables is a critical step in the development of a machine learning model. Thus, in the following sections, the details on the experimental database of RC beams with or without stirrups are provided. Moreover, the distribution of the database for both RC beams with and without stirrups is provided. The development of an accurate shear model requires the incorporation of all parameters affecting the shear capacity of RC beams. Thus, the input features (key design parameters) are identified and the effects of these factors on the response variable (shear capacity in this case) are discussed based on the collected database for both RC beams with/without stirrups in Section 3.1 and 3.2.

3.1 Experimental database for RC beams without stirrups

3.1.1 Introduction

A large superset database of RC beams without stirrups, which is collected by Collins et al. [41] is used in this study. The authors collected the test results of RC beams tested over 60 years of research between 1948 and 2006. A total of 1849 RC beams are contained in the database. The experimental database covers a wide range of beam geometries, material strengths (concrete and steel reinforcement), diameter and number of longitudinal reinforcement steel bars, and shear a/d ratios. The following general criteria were used to collect the database:

- Material strength: RC beams with no limit on the material strength, i.e., no limit on the f_c' and yield strength of longitudinal reinforcement bars. Details on the material strength will be provided in the subsequent sections.
- Beam shape: both rectangular and T-section beams are included in the database.
- Reinforcement: beams without stirrups.
- Concrete: normal strength concrete without additional fibers.
- Bar type: deformed longitudinal steel bars.
- Load type: point load or uniform load (details will be provided in the following subsection).
- Beam geometries: no limits on the geometric size of the beams.

As mentioned above, both RC rectangular and T-section beams are contained in the database. As shown in **Figure 3.1**, among the total of 1849 RC beams included in the database, 1599 beams were rectangular beams representing 86% of the beams, while 250 RC beams had T-section, which denotes 14% of the beams.

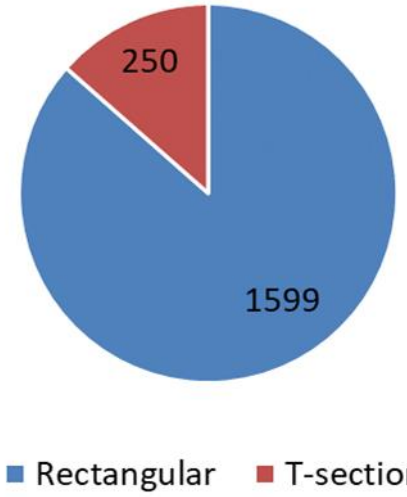

Figure 3.1: Geometry of RC beams in the database.

The beams were tested under three types of loading conditions: (a) point load (Type P), (b) uniform load with one concentrated load (Type U1), and (c) uniform load with two-point concentrated loads (Type U2). **Figure 3.2** shows the details of the three loading types.

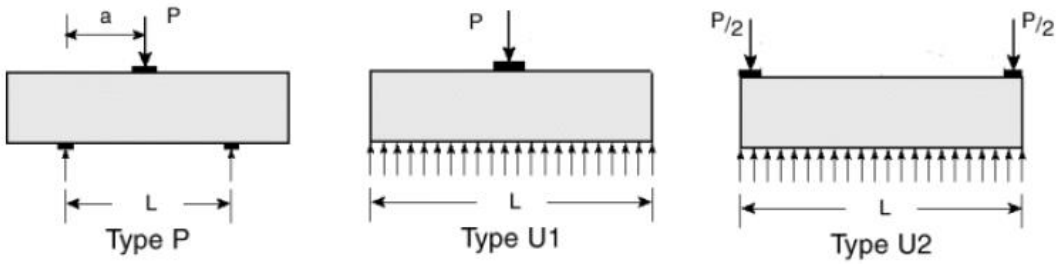

Figure 3.2: Schematic of the loading types

Figure 3.3 shows the distribution of the beams loading type. Among the total 1849 RC beams, 1701 beams were tested under three-point load (Type P), which represents 92% of the beams. Thus, the majority of the beams were tested under Type P loading condition.

For the uniform loads, 11% were tested under Type U1, while the remaining 3% were tested under Type U2 loading condition.

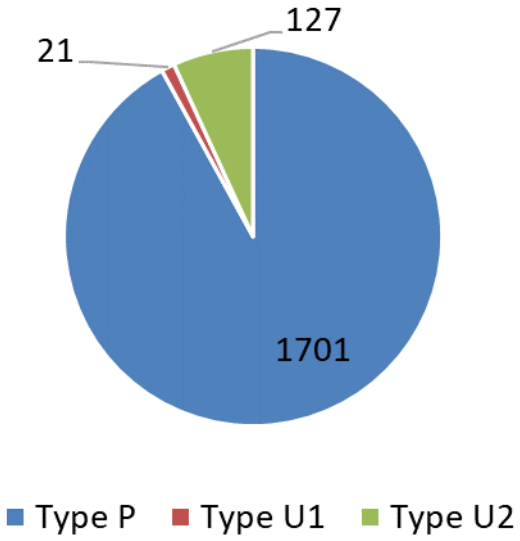

Figure 3.3: Distribution of RC beams in terms of the loading type.

As discussed earlier, the development of efficient machine learning models requires proper identification of the input features or key design parameters that influence the response variables; namely, the shear capacity of the beams in this case. In this study, a total of eight important factors are identified based on a thorough literature review. These factors include the width of the web (b_w), the width of the flange (b), cross-sectional depth (h), effective depth of the section (d), shear span-to-effective depth ratio (a/d), concrete compressive strength (f_c'), longitudinal reinforcement ratio (ρ_s), and yield strength of steel bars (f_y). The details on the distribution of these factors and their effect on the shear capacity are provided in the following sections.

3.1.2 Distribution of input parameters

A wide range of input parameters is comprised in the database. **Figure 3.4** shows the distribution of each factor. Moreover, the distribution of the input features in terms of the average (mean) value, standard deviation (STD), minimum, first quartile (Q1), second quartile (Q2), third quartile (Q3), and maximum values are listed in **Table 3.1**. As can be observed in **Figure 3.4** and **Table 3.1**, an extensive range of the factors is included in the database. For instance, the values of f_c' ranged between 6.1 MPa to 127.5 MPa with a mean strength of 34.86 MPa and a standard deviation of 18.34 MPa. As shown in **Figure 3.4** and **Table 3.1**, 75% of the beams were constructed with concrete having a compressive strength of 24.1 MPa or higher strength. The compressive strength of concrete in most of the beams ranged between 24.1 MPa and 50 MPa, as shown in **Figure 3.4**. With regard to the beam section, the width of the beam web and flange ranged between 21 mm to 3000 mm, the height of the beam section was in the range of 51 mm–3140 mm, and the effective depth of the beam ranged from 41 mm to 3000 mm, as listed in **Table 3.1**. Moreover, the a/d ratio is in the range of 0.25 to 15.06. Thus, both slender and deep beams are included in the database. As per the ACI- ASCE Committee 445 [53], RC beams with a/d ratio of

less than 2.50 are characterized as deep beams, while slender beams have a/d ratio of greater than 2.50.

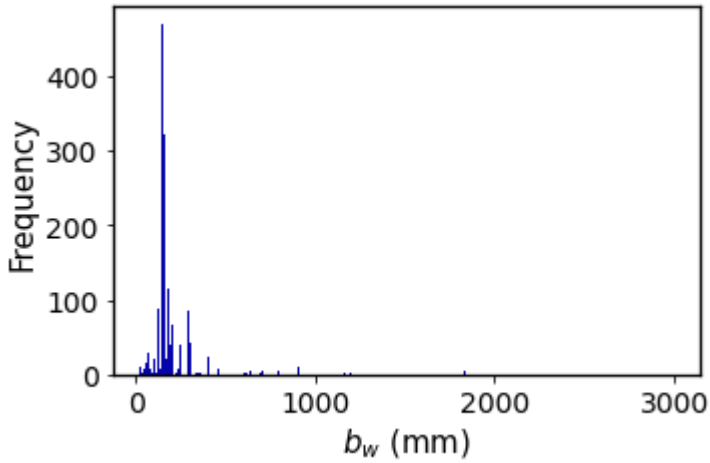

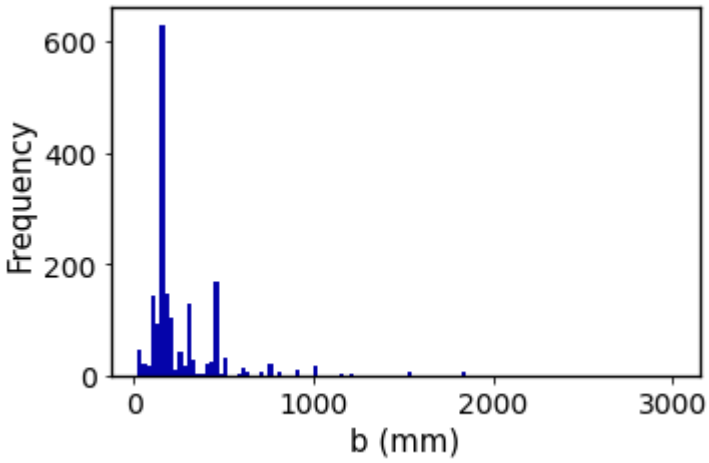

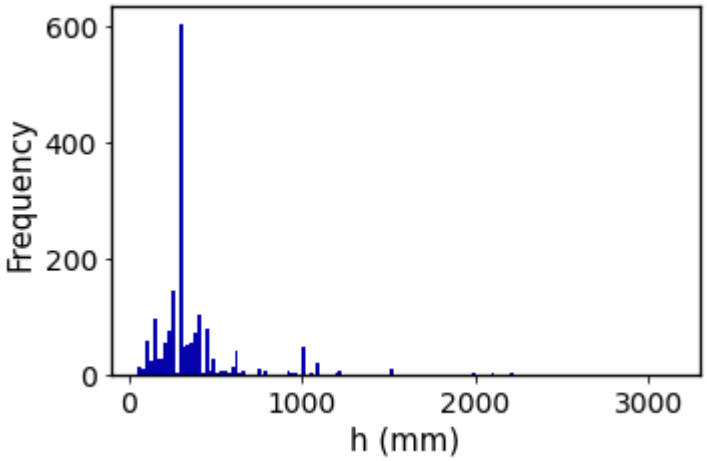

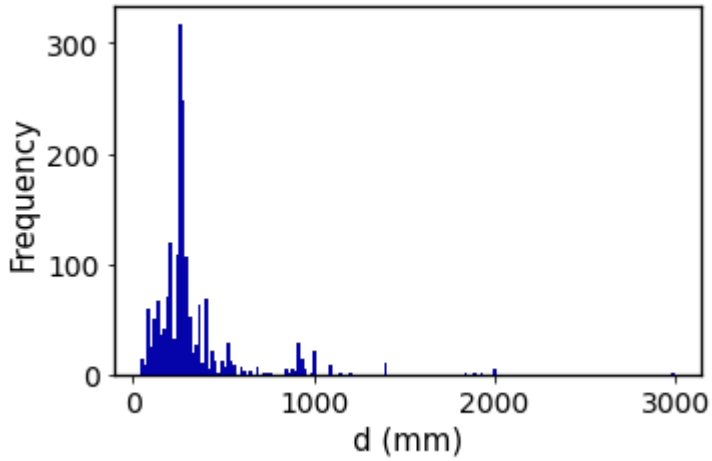
Frequency
300
200
100
0
0
1000
2000
3000
d (mm)

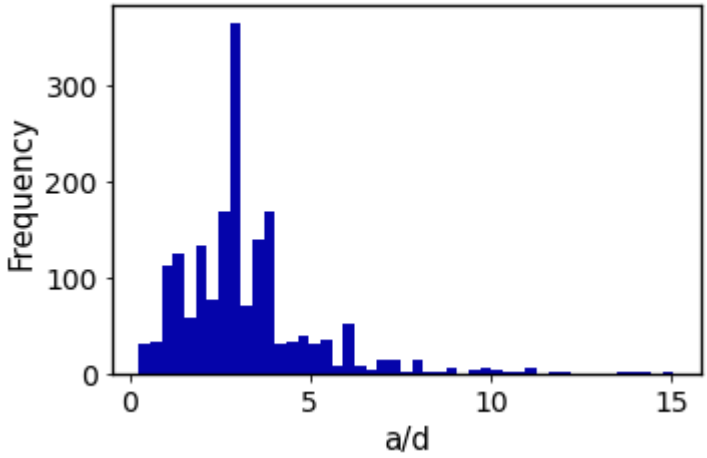
Frequency
300
200
100
0
0
5
10
15
a/d

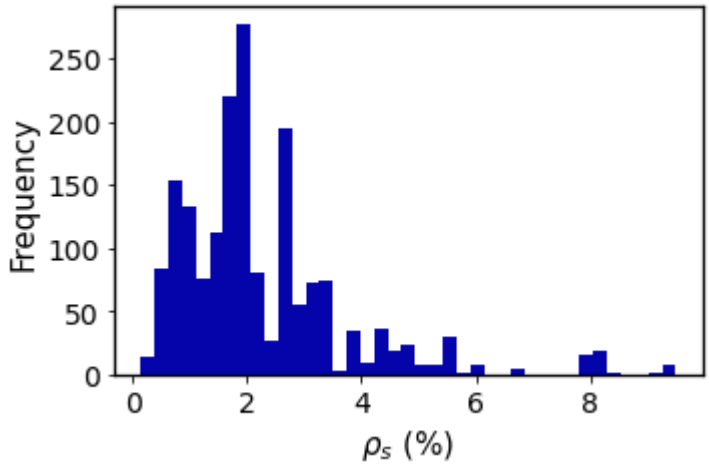
Frequency
250
200
150
100
50
0
0
2
4
6
8
ρ_s (%)

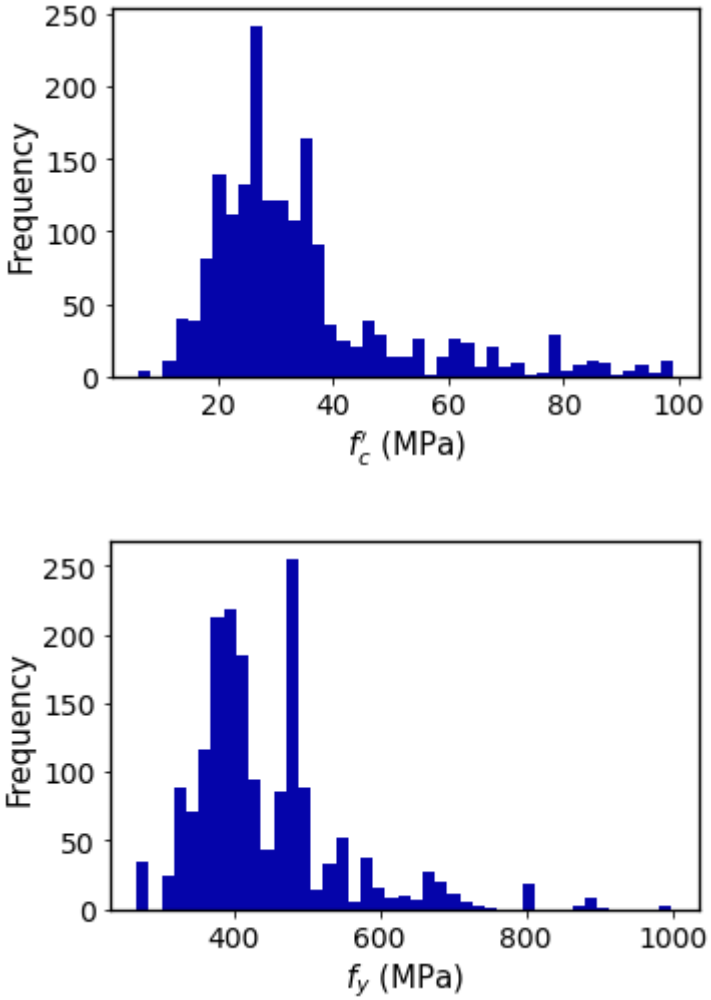

Figure 3.4: Distribution of the input variables in the database.

Table 3.1: Geometry and material characteristics of the beams included in the database

Parameters	Mean	STD	Minimum	Q1	Q2	Q3	Maximum
$b_w\ (mm)$	213.01	212.94	21	150	153	200	3000
$b\ (mm)$	256.76	230.21	21	152	157	300	3000
$h\ (mm)$	364.35	254.05	51	250	305	381	3140
$d\ (mm)$	320.25	237.77	41	210	270	318	3000

a/d	3.20	1.80	0.25	2	3	3.94	15.06
$f_c\ (MPa)$	34.86	18.34	6.1	24.1	29.7	37.4	127.5
$\rho_s\ (\%)$	2.24	1.52	0.1	1.24	1.87	2.73	9.5
$f_y\ (MPa)$	462.37	172.14	267	379	420	483	1779

STD: standard deviation

As discussed earlier, the flexural reinforcement bars had a deformed shape. The yield strength of flexural reinforcement bars ranged between 172.14 MPa to 1779 MPa, as listed in **Table 3.1**; however, most of the beams were reinforcement with flexural bars with yield strength in the range of 379 MPa–550 MPa, as shown in **Figure 3.4**. Finally, the longitudinal reinforcement ratio ranged between 0.1% and 9.5% with a mean value of 2.24% and standard deviation of 1.52%. It is worth mentioning here that the concrete compressive strength and yield strength of longitudinal reinforcement bars are limited to 100 MPa and 1000 MPa, respectively, in the final database used in the development of the machine learning-based models, as will be discussed further in Chapter 5. The effect of the input parameters on the shear capacity of RC beams is briefly discussed in the following section.

3.1.3 Effect of input parameters on the shear capacity

In Section 2.2, the effect of different key design factors on the shear capacity is discussed based on a thorough literature review. In this section, the collected database is used to investigate the influence of the factors on the shear capacity of RC beams without stirrups. **Figure 3.5** depicts the variation of the shear capacity (V_u) with the change in each factor based on the test results of RC beams included in the database.

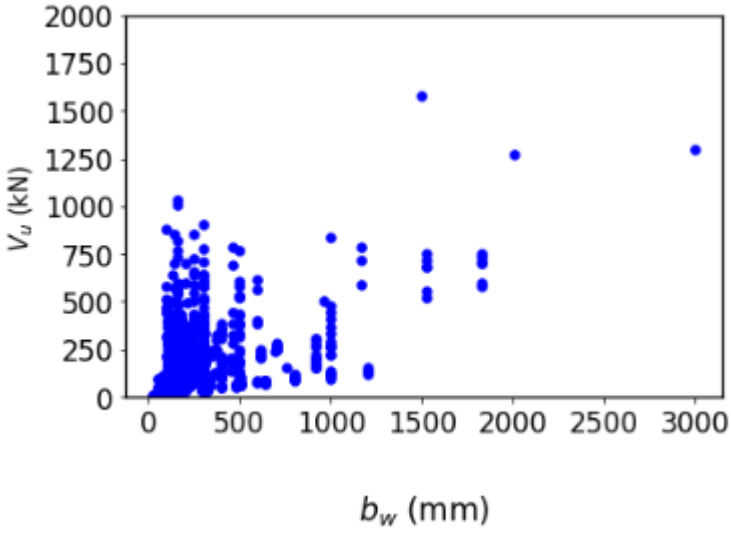
2000
1750
1500
1250
1000
750
500
250
0
V_u (kN)
0
500
1000
1500
2000
2500
3000
b_w (mm)

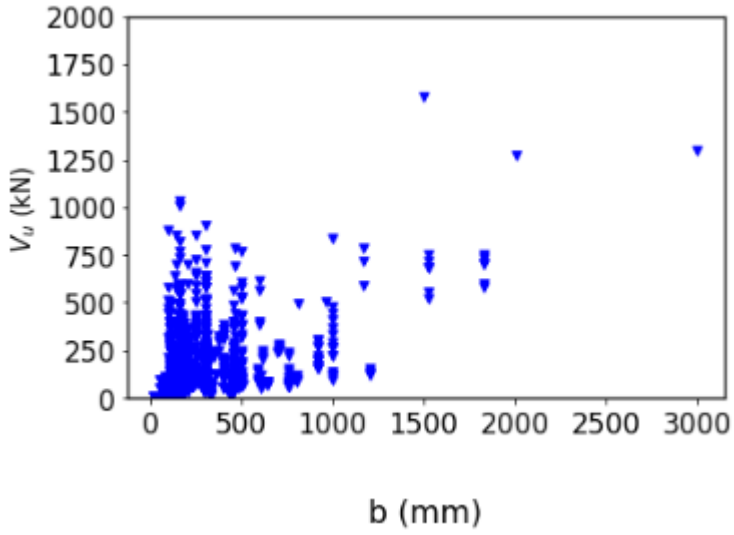
2000
1750
1500
1250
1000
750
500
250
0
V_u (kN)
0
500
1000
1500
2000
2500
3000
b (mm)

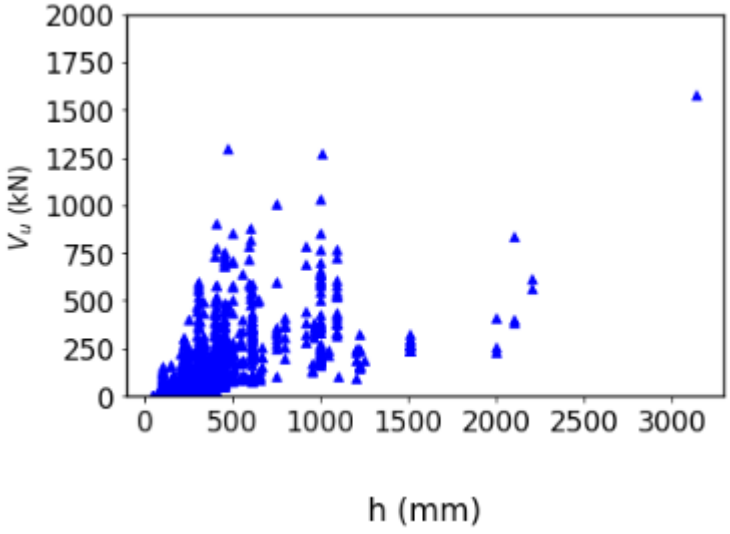
2000
1750
1500
1250
1000
750
500
250
0
V_u (kN)
0
500
1000
1500
2000
2500
3000
h (mm)

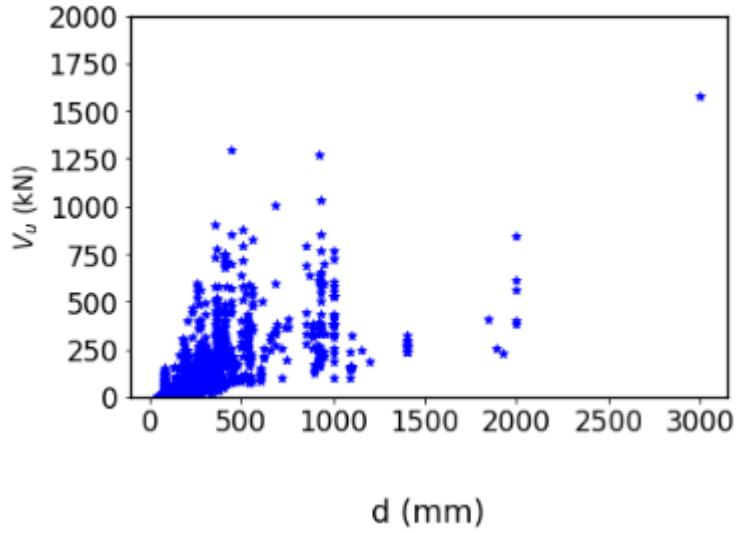
2000
1750
1500
1250
1000
750
500
250
0
V_u (kN)
0
500
1000
1500
2000
2500
3000
d (mm)

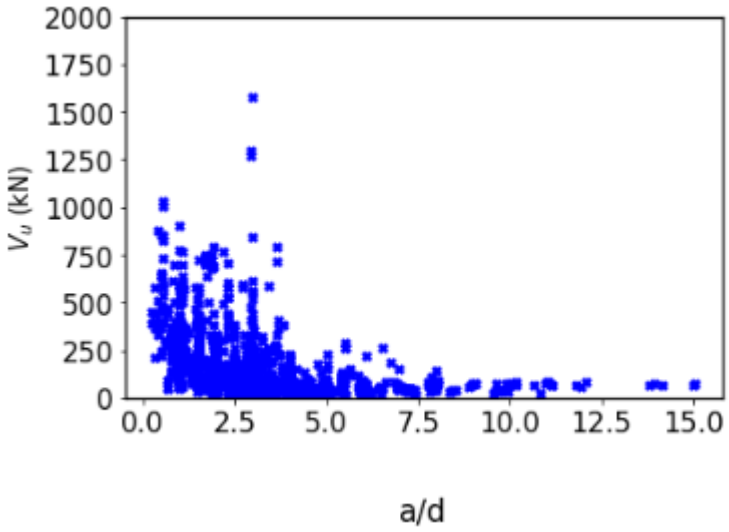
2000
1750
1500
1250
1000
750
500
250
0
V_u (kN)
0.0
2.5
5.0
7.5
10.0
12.5
15.0
a/d

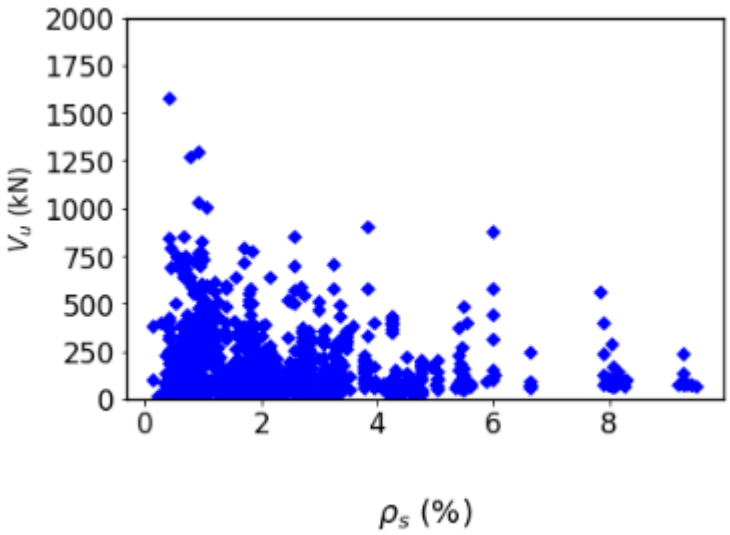
2000
1750
1500
1250
1000
750
500
250
0
V_u (kN)
0
2
4
6
8
ρ_s (%)

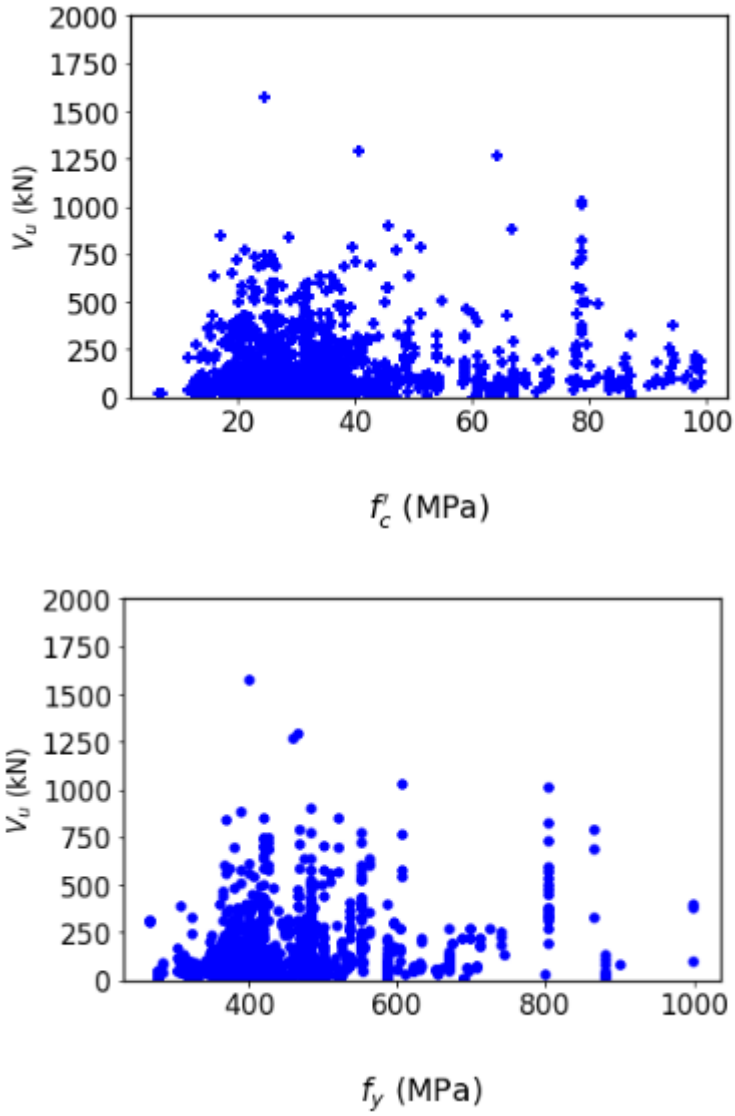

Figure 3.5: Relationship between the input parameters and the shear capacity.

As can be observed in **Figure 3.5**, each parameter significantly influences the shear capacity of RC beams. Moreover, there exists a nonlinear relationship between the factors and the shear capacity of RC beams. Thus, a simple linear model cannot be used to determine the shear capacity of the beams. Generally, the shear capacity of the beam increased with an increase in the width of the web, width of flange, height of the beam section, and effective depth of the beam, as shown in **Figure 3.5**. However, an increase in

the shear span-to-effective depth showed a negative effect on the shear capacity, thus, the shear capacity decreased with an increase in a/d ratio. The concrete compressive strength, yield strength of longitudinal bars, and reinforcement ratio of longitudinal bars showed a complex trend, which shows the complex nonlinear relationship between the factors and the shear capacity of the beams and interaction between the factors.

3.2 Experimental database for RC beams with stirrups

3.2.1 Introduction

A database of RC beams with stirrups, which is collected by Zhang et al. [42], Jung et al. [63], and Cladera et al. [64] is used in this study. The authors collected the experimental results of a total of 348 RC beams. The experimental database covers a wide range of beam geometries, concrete and steel reinforcement strengths, diameter and number of longitudinal and transversal reinforcement steel bars, and shear span-to-effective depth ratios. Both rectangular and T-section beams are included in the database. And also both slender beam and deep beam are included in the database. As shown in **Figure 3.6**, among the total of 348 RC beams included in the database, 116 beams were slender beams representing 33.33% of the beams, while 232 RC beams had deep beam, which denotes 66.67% of the beams.

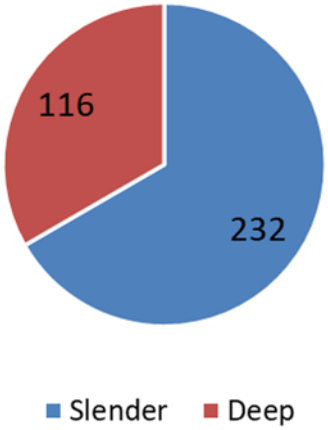

Figure 3.6: Beam type (slender beams/deep beams)

As discussed in section 4.1, the development of efficient machine learning models requires proper identification of the input features or key design parameters that influence the response variables; namely, the shear capacity of the beams in this case. In this study, a total of seven important factors (input features) are identified based on a thorough literature review. These factors include the width of the flange (b), effective depth of the section (d), shear span-to- depth ratio (a/d), compressive strength of concrete (f_c'), reinforcement ratio of longitudinal bars (ρ_{sy}), transversal reinforcement ratio (ρ_{sy}), and yield strength of steel bars (f_y). The details on the distribution of these factors and their influence on the shear capacity are provided in the following sections.

3.2.2 Distribution of input parameters

Figure 3.7 illustrates the distribution of each input parameters. Moreover, the distribution of the input features are listed in **Table 3.2**. As can be observed in **Figure 3.7 and Table 3.2**, an extensive range of the factors is included in the database. The values of f_c' ranged between 12.8 MPa to 125 MPa with an average strength of 41.21 MPa and a standard deviation of 20.67 MPa, the yield strength of flexural reinforcement bars ranged between

0 MPa to 844 MPa, the longitudinal reinforcement ratio ranged between 0.76 MPa and 5.8 MPa with a mean value of 2.86 MPa, and standard deviation of 0.97, and the transversal reinforcement ratio range between 0 MPA and 1.90 MPa, with a mean value of 0.31 MPa, and standard deviation of 0.23 MPa, With regard to the beam section, the width of the beam ranged between 76 mm to 457 mm, and the effective depth of the beam ranged from 95 mm to 1200 mm, and the shear span-to-effective depth ratio is in the range of 1 to 5.98, both slender and deep beams are included in the database, as listed in **Table 3.2**.

Table 3.2: Geometry and material characteristics of the beams included in the database

Parameters	Mean	STD	Minimum	Q1	Q2	Q3	Maximum
$b\ (mm)$	221.39	80.70	76.00	152.00	203.00	290.00	457.00
$d\ (mm)$	365.07	151.38	95.00	292.00	345.00	425.00	1200.00
a/d	2.98	0.82	1.00	2.50	3.00	3.60	5.98
$f_c\ (MPa)$	41.21	20.67	12.80	26.20	33.30	50.00	125.00
$\rho_{sx}\ (\%)$	2.86	0.97	0.76	2.20	2.80	3.40	5.80
$\rho_{sy}\ (\%)$	0.31	0.23	0.00	0.14	0.24	0.50	1.90
$f_y\ (MPa)$	423.74	146.08	0.00	331.00	379.00	531.00	844.00

STD: standard deviation; Q1: first quartile; Q2: second quartile; Q3: third quartile

In the final database used in the development of the machine learning-based models, as will be discussed further in Chapter 6. The effect of the input parameters on the shear capacity of RC beams is briefly discussed in the following section

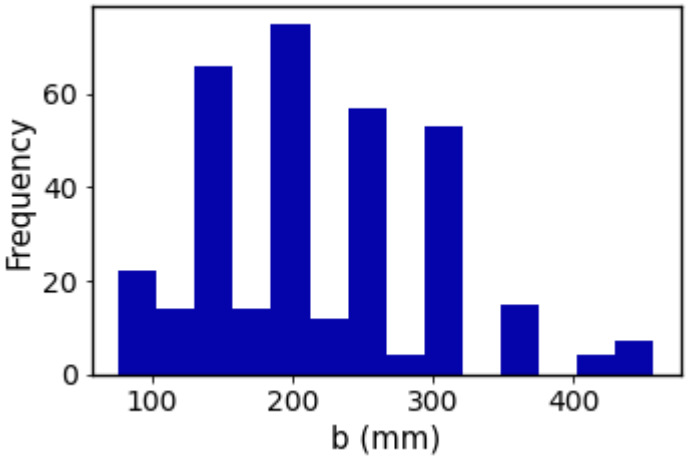
Frequency
0
20
40
60
100
200
300
400
b (mm)

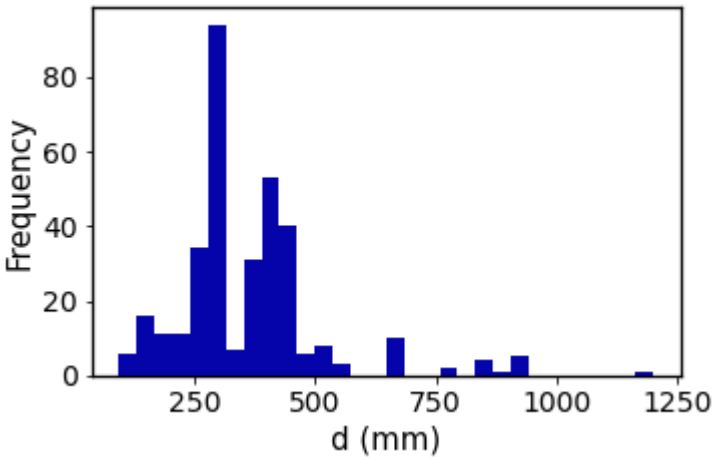
Frequency
0
20
40
60
80
250
500
750
1000
1250
d (mm)

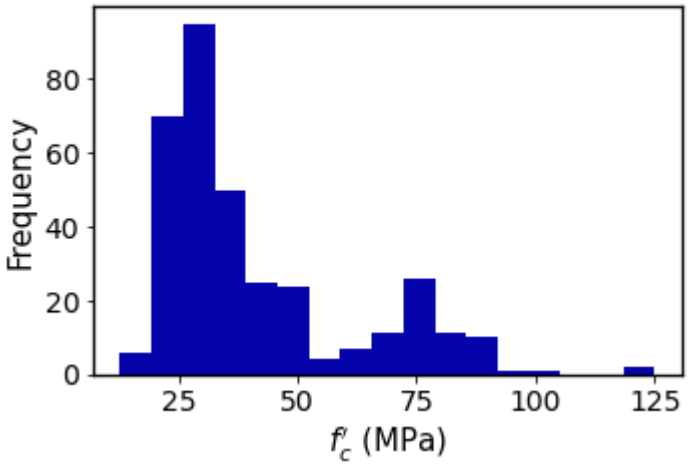
Frequency
0
20
40
60
80
25
50
75
100
125
f'_c (MPa)

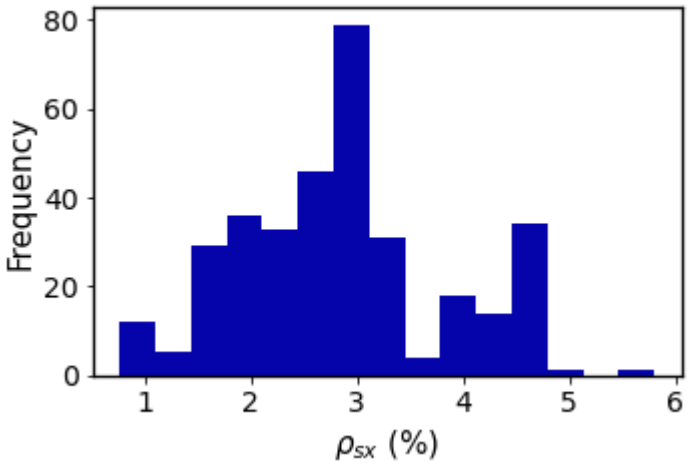
Frequency
80
60
40
20
0
1
2
3
4
5
6
ρ_{sx} (%)

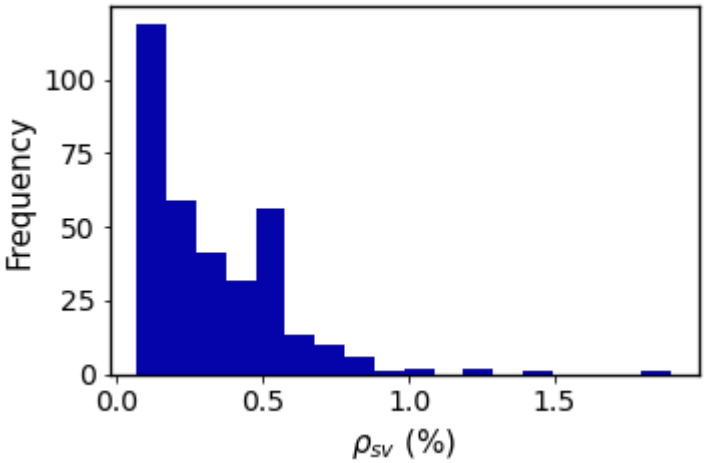
Frequency
100
75
50
25
0
0.0
0.5
1.0
1.5
ρ_{sv} (%)

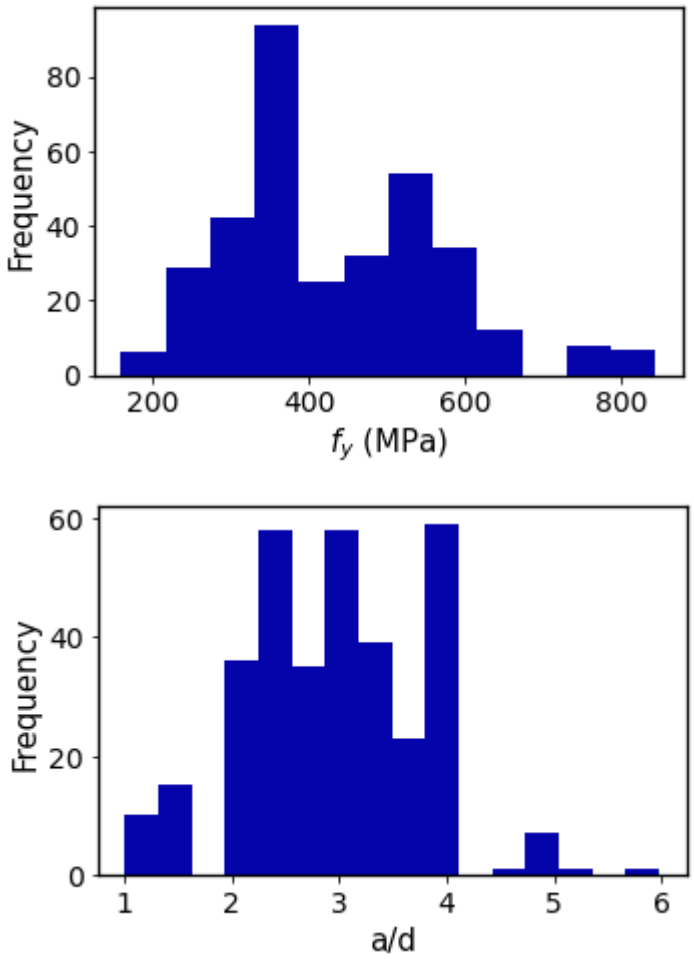

Figure 3.7: Distribution of the input variables in the database.

3.2.3 Effect of input parameters

In this section, the collected database is used to investigate the influence of the factors on the shear capacity of RC beams with stirrups. **Figure 3.7** shows the variation of the shear capacity (V_u) with the change in each factor based on the experimental results of RC beams included in the database.

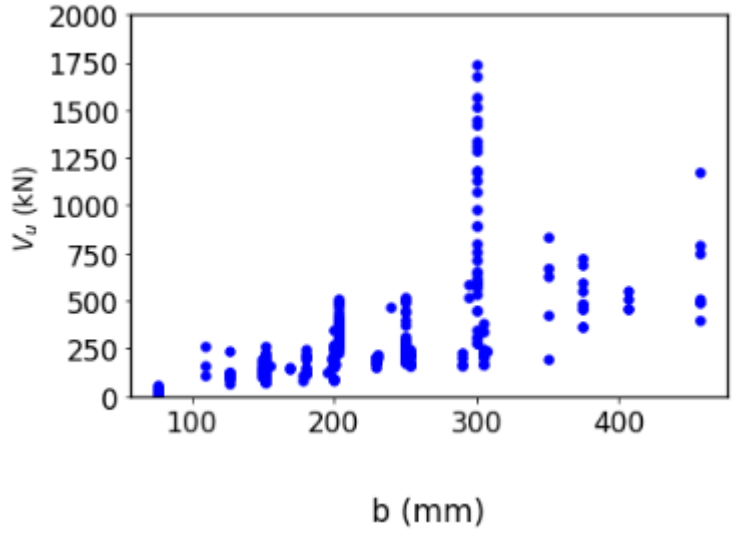
2000
1750
1500
1250
1000
750
500
250
0
V_u (kN)
100
200
300
400
b (mm)

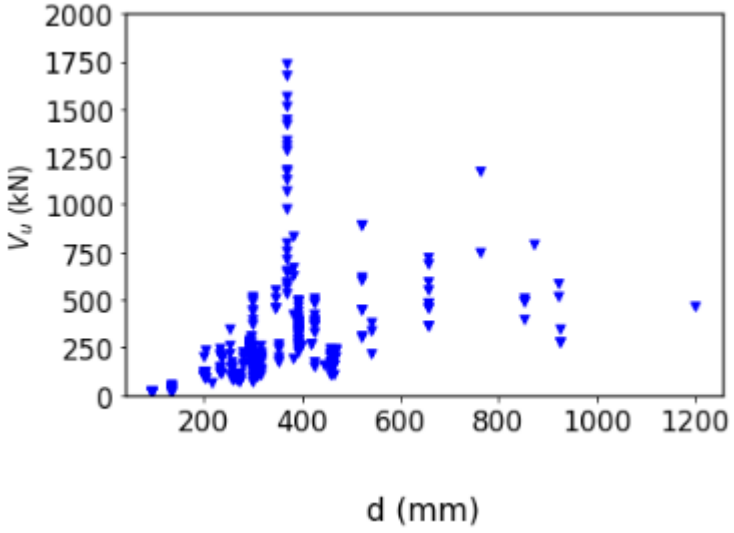
2000
1750
1500
1250
1000
750
500
250
0
V_u (kN)
200
400
600
800
1000
1200
d (mm)

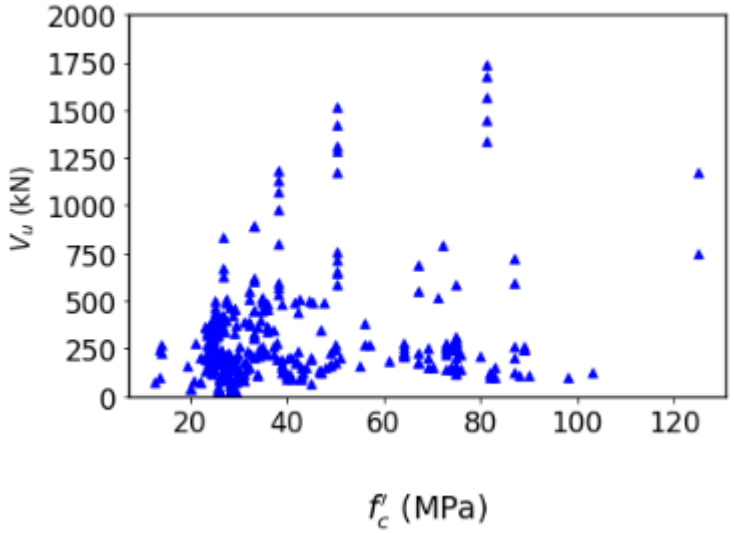
2000
1750
1500
1250
1000
750
500
250
0
V_u (kN)
20
40
60
80
100
120
f'_c (MPa)

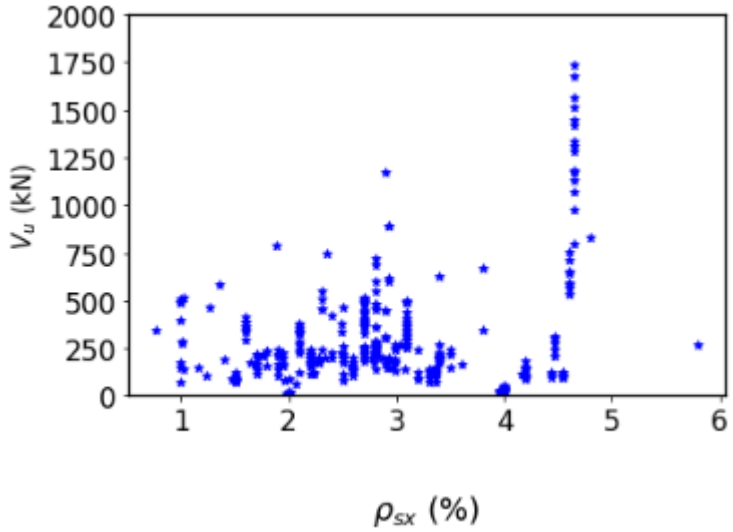
2000
1750
1500
1250
1000
750
500
250
0
V_u (kN)
1
2
3
4
5
6
ρ_{sx} (%)

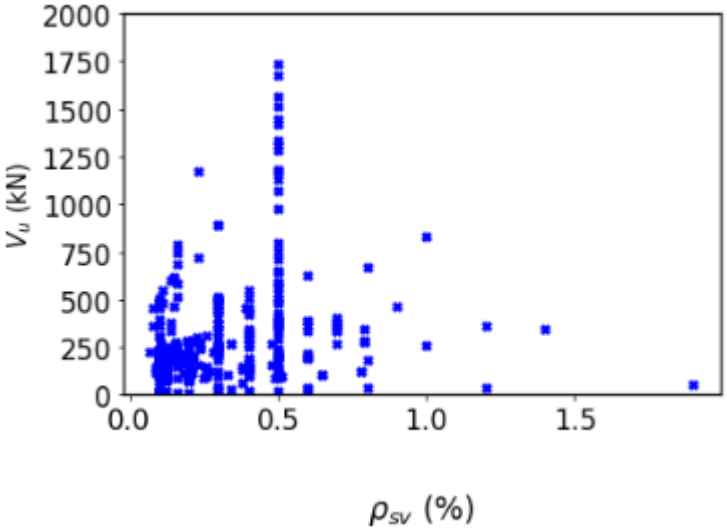
2000
1750
1500
1250
1000
750
500
250
0
V_u (kN)
0.0
0.5
1.0
1.5
ρ_{sv} (%)

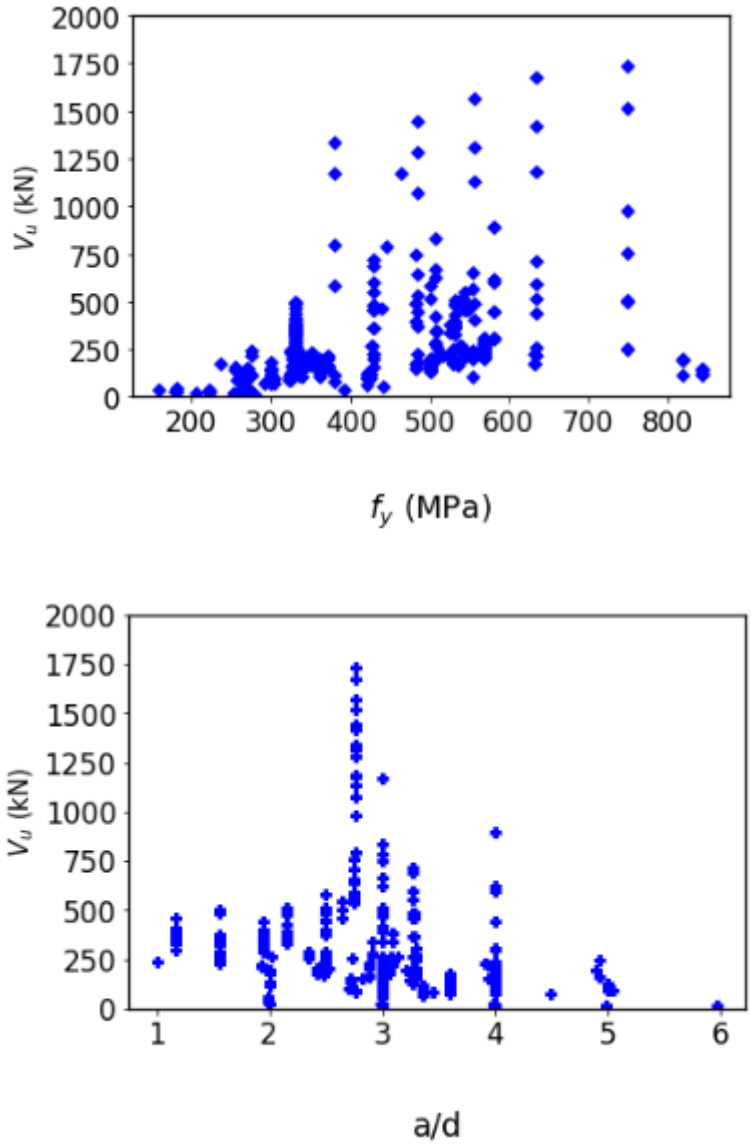

Figure 3.8: Relationship between the input parameters and the shear capacity of RC beams with stirrups

As observed from **Figure 3.8**, all parameter significantly influences the shear capacity of RC beams and there is the complex nonlinear relationship between the factors and the shear capacity of the beams and interaction between the factors.

CHAPTER 4 MACHINE LEARNING-BASED MODELS

4.1 Introduction to Machine Learning

Machine learning has recently gained immense attention owing to its ability to effectively determine the relationship between the input features and the response variable (s) in a complex system. In contrast to the case of most empirical models, ML techniques does not require the prior assumption or knowledge of the underlying mathematical and physical models [16]. Artificial neural network (ANN) is one of the most widely utilized ML techniques [9]. It has been successfully employed for different structural engineering studies; some of which include the prediction of mechanical properties of concrete [6,8–10], damage assessment of bridges [22–24] and buildings [25], ultimate deformation capacity of RC columns [11], shear strength of circular RC columns [26], and compressive strength [13–15] and the stress-strain relationship [12] of concrete confined with FRP. ANN has also proved to be able to predict the shear capacity of pristine [35,39,65] and FRP strengthened [66,67] RC beams. A review of the application of different artificial intelligent techniques in structural engineering is conducted by Salehi and Burgueño [5]. Support vector machine (SVM) is another powerful ML technique that has been applied to structural engineering problems [27–29]. Solhmirzaei et al. [29] used three different ML techniques, namely, SVM, k-nearest neighbor (kN), and ANN to predict the failure modes of Ultra High Performance Concrete (UHPC) beams. The results showed that ANN outperformed the other two methods in predicting the failure modes of UHPC beams with an overall accuracy of 89%.

Ensemble models are another type of emerging ML technique in the field of structural engineering with high performance. These algorithms combine two or more learners known as base learners (e.g. kernel regression, support vector machine, and decision tree) in order to improve the prediction performance, robustness, and stability of the base learners [30]. Ensemble learners can be formed in sequential or parallel styles with the aim to exploit the dependence and independence between the base models, respectively. Bagging (short for **B**ootstrap **Agg**regating) [31] is one of the ensemble models in which multiple base learners are independently trained in parallel using different bootstrap sample. Each bootstrap training dataset contains an average of 63.2% of the original training set. The final prediction is then taken as the mean of the predictions from the base learners [31]. As a result a better prediction with reduced variance is obtained [31]. Random forest (RF) is a popular example of bagging ensemble learners. In RF homogeneous base learners, particularly, decision trees are used. An ensemble model can also be formed from multiple base learners of different types or heterogeneous base learners [30]. Stacking ensemble is one of the heterogeneous ensemble models in which different types of base learners are combined via a meta-model with the objective of enhancing the accuracy of the individual model [32,33].

In the previous study, different researchers have attempted to examine the efficacy of ML models to estimate the capacity of RC beams in shear [34–39]. However, generally, a limited number of experimental databases were used in the previous study. Moreover, despite the investigation of the application of ML techniques to predict the capacity of RC beams in shear, all previous studies generally failed to propose a user-friendly and practical shear design approach based on the results of the trained ML models. As it is well

understood, ML algorithms are generally black-boxes and as such cannot be reproduced by others. Thus, practical implementation and simplification of the ML-based models are essential. Moreover, most of the models are developed using a limited number of experimental datasets, which limits the generalization of the developed models.

In lieu of the above-mentioned limitations, the current study investigated the application of several ML models (both single and ensemble models) to propose the best predictive model based on a large database of slender and deep RC beams with/without stirrups. Four types of homogeneous ensemble models that are based on decision trees; namely, random forest, gradient boosting, extremely randomized trees, and extreme gradient boosting (xgBoost) are considered. The xgBoost model, which is a comparatively new algorithm, uses regularization parameters in order to overcome the overfitting problem [68]. It has recently become popular across multiple disciplines [17,69–76].

Thus, this study adopted different advanced ensemble ML techniques, arguably for the first time, to predict the shear capacity of RC beams. Furthermore, the prediction capability of the ensemble models is compared with that of the base learners including support vector regression and decision tree. The proposed model has been compared against the existing models and code equations. The results of the analysis evidenced that the proposed model is superior to other existing models and guidelines in predicting the RC beam shear capacity. Finally, the best model among the developed models is deployed into a user-friendly web-based application, which can be used by practitioners and researchers in the field of civil engineering to accurately determine the capacity of RC beams in shear. The developed web-based application facilitates a rapid and accurate prediction of the capacity of RC beams in shear.

4.2 Normalization of dataset

To overcome the problems related to low rate of learning at the extreme values, the dataset is normalized within a range of 0 and 1 as follow:

$$x_n = \frac{x_{orig} - x_{min}}{x_{max} - x_{min}} \tag{25}$$

where x_{orig} is the original value of the variable, while x_n is its corresponding normalized value and x_{min} and x_{max} are the minimum and maximum values of the variable, respectively.

4.3 Performance measurement

Different statistical indices are commonly used to evaluate the performance of ML-based models. The following four indices are used in this study; namely, root mean squared error (RMSE), mean absolute percentage error (MAPE), mean absolute error (MAE), and coefficient of determination (R^2). The performance indices are given as follows:

$$MAE = \frac{1}{n}\sum_{i=1}^{n}|y_i - \hat{y}_i| \tag{26a}$$

$$MAPE = \frac{100}{n}\sum_{i=1}^{n}\left|\frac{y_i - \hat{y}_i}{y_i}\right| \tag{26b}$$

$$RMSE = \sqrt{\frac{1}{n}\sum_{i=1}^{n}(y_i - \hat{y}_i)^2} \tag{26c}$$

$$R^2 = 1 - \frac{\sum_{i=1}^{n}(y_i - \hat{y}_i)^2}{\sum_{i=1}^{n}(y_i - \bar{y})^2} \tag{26d}$$

where y is the target response, $\hat{y}$ is the predicted response, and $\bar{y}$ is the mean of the responses.

4.4 Hyperparameter optimization

The performance of a given machine learning model depends on the values of its hyperparameters, which are parameters that control the learning process of ML models. In this study, the optimal hyperparameters are determined using grid search and K-fold cross validation. Following the normalization of the dataset and identification of the input and response vectors, the dataset is randomly divided into the training set and test set including 80% and 20% of the complete dataset, respectively, as shown in **Figure 4.1**.

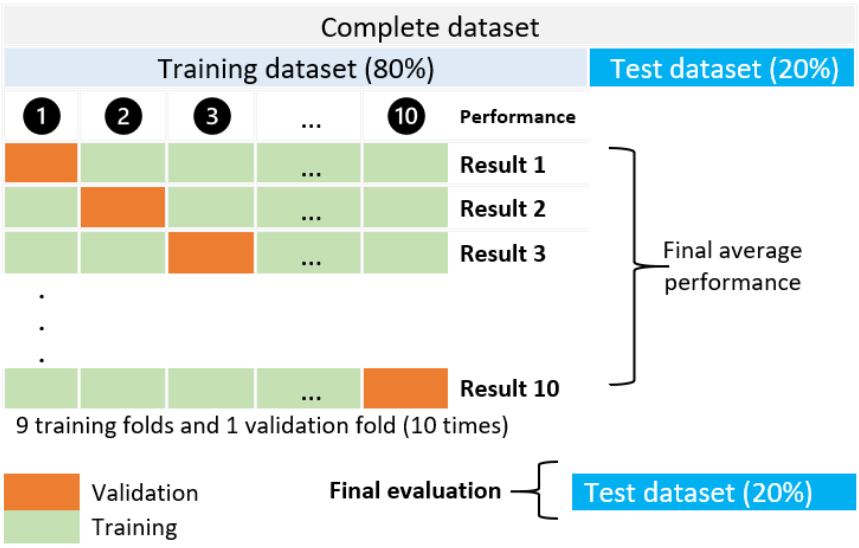

Figure 4.1: 10-fold cross-validation.

The ML model is trained on the training set, while the test dataset is used to finally appraise its performance. A standard *K*-fold cross-validation technique is adopted to evaluate the model, where *K* denotes the number of partitions. Here, the data is randomly split into *K* parts of equal sizes, and then the model is fitted on the $K-1$ parts, while the remaining one part is used to validate the model, as shown in **Figure 4.1** (for $K = 10$). Therefore,

each fold is used as a validation set and the cross-validation is repeated K times. The performance of the model is then determined as the average of the results from the K data folds, as illustrated in **Figure 4.1**. This study adopted a ten-fold ($K = 10$) cross-validation, as shown in **Figure 4.1**. The training of each model is performed using scikit learn [77], which is a powerful ML packing in python programming language. **Figure 4.2** summarizes procedures followed in the development of the ML models.

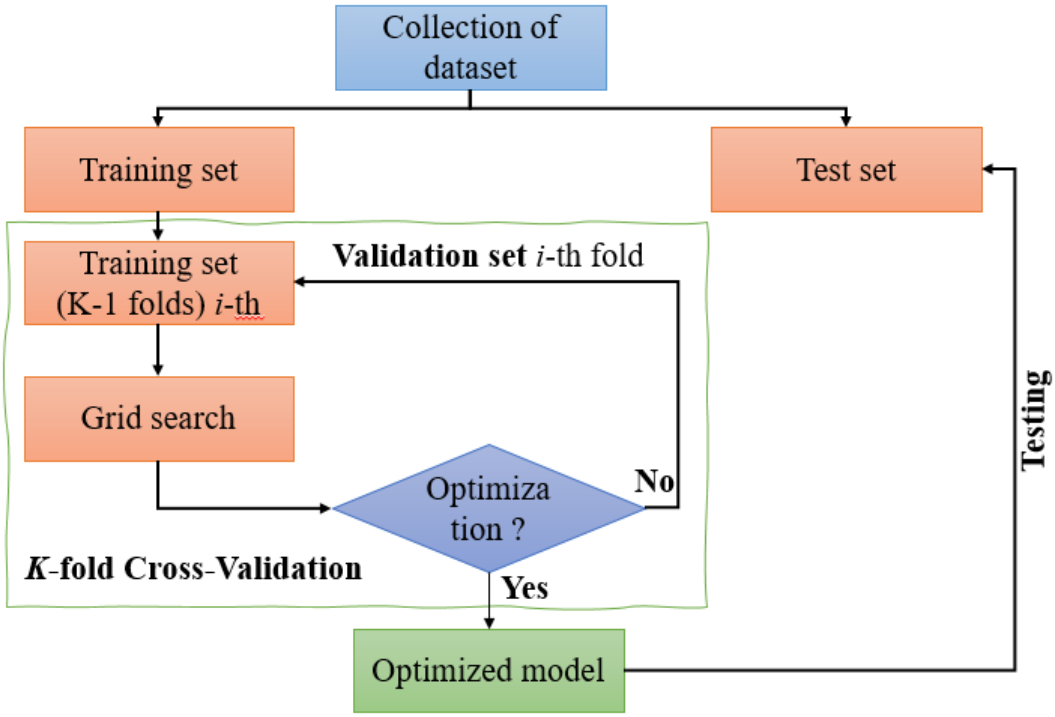

Figure 4.2: model development

4.5 Single ML models

4.5.1 Support vector machine

Support vector machine is one of the supervised ML techniques with associated algorithms primarily applied for classification problems using structural risk minimization principle

[78]. The SVM-based classifications are based on the optimal separation of classes. The algorithm in the SVM finds a hyperplane or decision surface that distinctly classifies the data points. It can also be used to efficiently perform both linear and non-linear regression by indirectly mapping the original input vectors into a very high-dimensional feature space in which they become separable, using kernel functions [78]. Different kernel functions can be used for SVM with the radial basis function (RBF) kernel being the most popular type. The RBF kernel, $K_{RBF}(X_1, X_1)$, on two vectors X_1 and X_2 is defined as follows:

$$K_{RBF}(X_1, X_1) = exp(-\gamma \|X_1 - X_2\|^2) \quad \textbf{(27)}$$

where $\gamma = 0.5/\sigma^2$ is a parameter that defines the spread of the kernel.

The other two types of nonlinear kernels used in SVM include sigmoid and polynomial kernels defined as follow:

$$K_{sigmoid}(X_1, X_2) = \tanh(\gamma \langle X_1, X_2 \rangle + r) \quad \textbf{(28)}$$

$$K_{polynomial}(X_1, X_2) = (\gamma \langle X_1, X_2 \rangle + r)^d \quad \textbf{(29)}$$

The above three nonlinear kernel functions; namely, polynomial, RBF, sigmoid kernels are considered in this study. The other two hyperparameters that greatly affect the SVR predictive capacity are the regularization parameter C and ε-insensitive zone [79]. These hyperparameters are also optimized in this study.

4.5.2 Decision tree

Decision tree also referred to as classification and regression tree (CART) is a supervised ML algorithm that is similar to a flowchart-like structure. It is a tree-structured model with three types of nodes; the root node, interior node, leaf node (terminal node) as showed in **Figure 4.3**. The CART method splits the feature space into multiple smaller disjoint

regions with similar response values using a set of rules to predict a class label (in classification) and value (in regression) of the response variable. Each internal node in CART specifies a test on an attribute of the data, while each branch represents the test output. The root node, which is the topmost node in CART denotes the most relevant feature, while the leaf node or terminal node provides the predicted response variable.

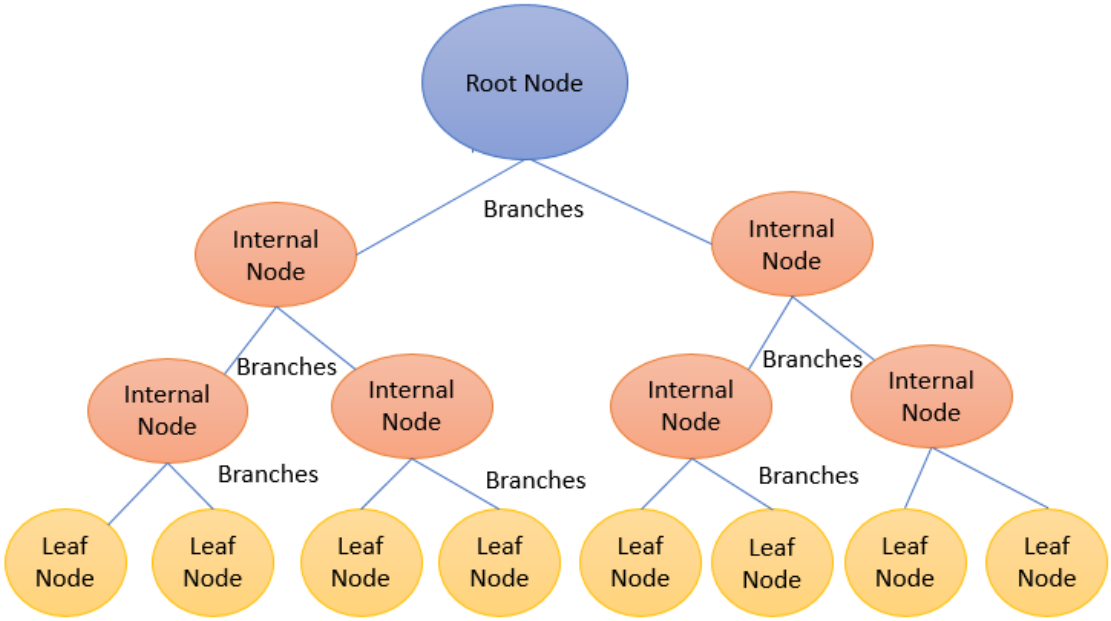

Figure 4.3: Decision tree flow chart.

The performance of CART model can be optimized by tuning its hyperparameters including the maximum depth of the tree, minimum samples number needed to be at a leaf/terminal node, and minimum number of samples required to split an internal node.

Decision tree algorithm is easy to visualize and interpret; however, it has less generalization ability, high bias, and high variance. Ensemble models can be used to overcome the problems associated with a single decision tree as discussed below.

4.6 Ensemble Models

Ensemble learners are supervised machine learning paradigm that combine multiple single learners (a.k.a. weak learners or base learners) into one predictive model to decrease variance error, bias, and produce a strong model with enhanced generalization capability and superior performance [80]. The basic idea behind the ensemble model is to combine multiple base learners in computing the final response rather than relying on an individual model. The ensemble models can be formed in either parallel or sequential manner. Moreover, ensemble models can be formed from homogeneous base learners (same type of base learner algorithms) or heterogeneous base learners (different types of base learner algorithms).

The most popular type of meta-algorithms that combines base learners are bootstrap aggregation (bagging) [31] and boosting [81] ensembles. In bagging ensemble (e.g., random forest), multiple base learners are independently trained in parallel mode on a different bootstrap sample, while in boosting ensemble (e.g., gradient boosting) the base models are trained sequentially.

4.6.1 Random forest

Random forest (RF) is a forest of randomly created CART models. It is the most used type of tree-based ensemble. It randomly combines two or more decision trees to make a decision [82]. However, it uses a bootstrap sample to train a series of decision trees and make the final prediction unlike a single decision tree that is construct using the complete training dataset [83]. It has emerged as a versatile and highly accurate methodology to solve both classification as well as regression problems and with a capability to handle

large features with a small sample size and reduce the variance of prediction while keeping low bias [82,84,85]. In this study, RF is combined with 10-fold cross-validation which further acts to prevent overfitting.

Figure 4.4 shows the training process involved in random forest regression. Given training dataset $\{(x_1, y_1), (x_2, y_2), \dots, (x_n, y_n)\}$ with n observations, where $x_i \epsilon X = \langle x_{i,1}, x_{i,2}, \dots, x_{i,j} \rangle \subseteq R^j$ are j independent variables and $y_i \epsilon Y \subseteq R$ is the response parameter. The RF creates N numbers of bootstrap sample (S) and trains N number of decision trees each bootstrap sample, as can be observed in **Figure 4.4**. The final prediction is then obtained as the average of the predictions from each decision tree, **Figure 4.4**.

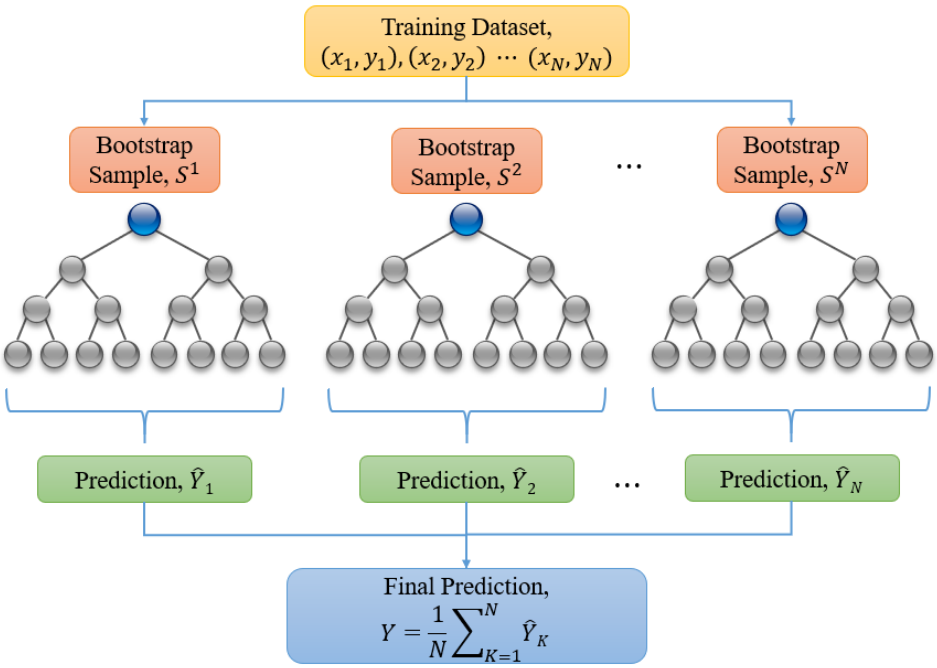

Figure 4.4: Conceptual schematic of random forest.

4.6.2 Extremely Randomized Trees

An additional type of ensemble learner referred to as extremely randomized trees (ERT) was proposed by Geurts et al. [86]. It can be applied to solve classification as well as regression based problems. Extremely randomized trees differs from random forest in two major features. Firstly, each decision tree in ERT is trained using the entire dataset in contrast to random forest algorithm that uses a bootstrap sample. Secondly, ERT adds randomization in selecting the split points of each node [86]. Similar type of hyperparameters as that of random forest are used in extremely randomized trees. However, the hyperparameters are independently tuned for both random forest and extremely randomized trees.

4.6.3 Gradient boosting

Gradient boosting machine is a powerful boosting algorithm, which combines a sequence of weak learners to generate an additive model whose performance is significantly enhanced compared to the base learners [87]. Similar to other boosting algorithms, gradient boosting regression (GBR) trains multiple learners sequentially. Given a training examples $X = \{(x_1, y_1), (x_2, y_2), \dots, (x_n, y_n)\}$, the GBR fit the model $F_m(x)$ using M trees [88]:

$$F_m(x) = F_{m-1}(x) + h_m(x) \quad \textbf{(30)}$$

$$h_m = \arg\min_h \left[\sum_{i=1}^{n} L(y_i, F_{m-1}(x_i) + h(x_i)) \right] \quad \textbf{(31)}$$

where h_m is the m^{th} tree and F represents set of all possible trees.

The objective of a newly added decision tree at each iteration is to reduce the loss given by:

$$\vartheta_m = -\frac{\partial[y, F_{m-1}(x)]}{\partial F_{m-1}(x)} \tag{32}$$

Where ϑ_m is the loss function.

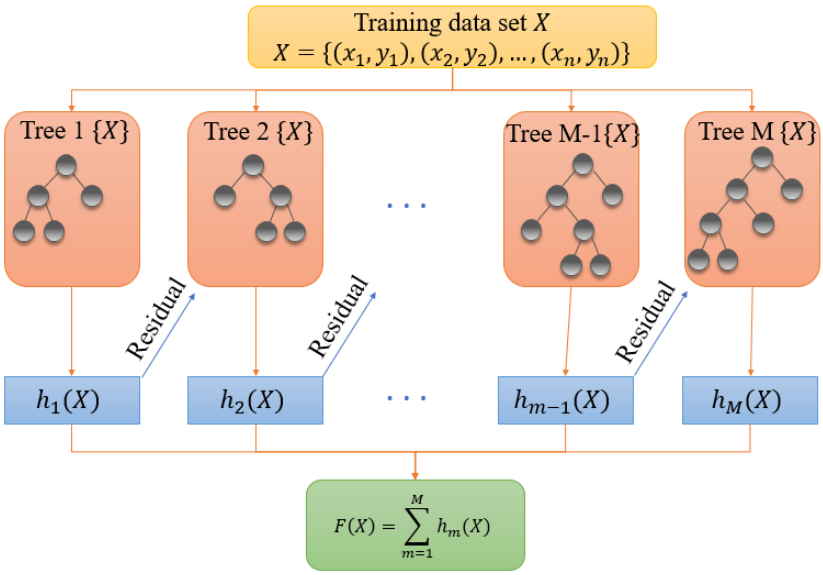

Figure 4.5: Conceptual schematic of gradient boosting.

4.6.4 Extreme gradient boosting

In 2016, Chen and Guestrin [68] proposed an enhanced form of gradient boosting algorithm know as extreme gradient boosting (xgBoost). The main difference of the xgBoost from the gradient boosting is in its objective function. The xgBoost algorithm adds a regularization parameter to reduce complexity of the model and produce a better generalization ability [68]. Its objective function (J) is given as follows in which the regularization term (Ω) controls the complexity of the model [68]:

$$J = \sum_i L(\hat{y}_i, y_i) + \sum_m \Omega(f_m) \tag{33}$$

The regularization parameter is determined as follows [68]:

$$\Omega(f_m) = \gamma M + \frac{1}{2}\lambda\|\omega\|^2 \quad \textbf{(34)}$$

where M is the number of decision trees, γ and λ are the regularization coefficients, and ω is the internal split tree weight.

CHAPTER 5 RESULTS AND DISCUSSION

5.1 RC beams without stirrup

The first step in the development of machine learning model is data collection and preprocessing including normalization of dataset. As discussed in preview chapter, the dataset is randomly partitioned into the train and test sets, which comprises 80% of the dataset for training and 20% of the dataset for testing. The training set is used to train and develop the models, while the test set is used to finally appraise the models based on different performance indices. During the model development, the hyperparameters of each model are tuned to find the most powerful and best model. The results of hyperparameter tuning are summarized in Table 5.1.

Table 5.1: Optimized hyperparameters for each model for RC beams without stirrup

Models	Optimum parameters
SVR	Kernel type = radial basis function, C = 600, ε = 0.01
CART	Maximum depth = 7, maximum features = 5, minimum sample leaf = 1, minimum sample split = 3
RFR	Number of estimators = 17, depth_max = 10, features_max = 5, minimum sample leaf = 1, minimum sample split = 2
ERT	Number of estimators = 33, maximum depth = 10, maximum features = 8, minimum sample leaf = 1, minimum sample split = 2
GTBR	Number of estimators = 62, learning rate = 0.15, depth_max = 7, subsample = 0.3, features_max = 5, minimum sample split = 2

xgBoost	Number of estimators = 180, learning rate = 0.15, maximum depth = 7, subsample = 0.3

The models are train in train dataset and tested in test dataset, as described in previous chapter six models (two single models and three ensemble models) namely; support vector machine, decision tree, random forest, extremely randomized tree, gradient boosting and extremely gradient boosting are included in the study. The result from each model for both train and test dataset in terms of performance indices; MAE, MAPE, RMSE, R^2 for RC beam without stirrup are discussed in Table 5.2.

Table 5.2 : Performance indices for RC beams without stirrup

Model	Training dataset				Test dataset			
	MAE	MAPE	RMSE	R2	MAE	MAPE	RMSE	R2
SVR	30.081	0.359	56.378	0.872	29.100	0.382	56.274	0.836
CART	27.855	0.308	45.552	0.917	33.060	0.348	57.416	0.830
RFR	14.713	0.130	27.902	0.969	20.813	0.170	42.548	0.906
ETR	16.296	0.202	25.873	0.973	21.787	0.234	41.848	0.910
GBR	12.197	0.142	18.698	0.986	17.305	0.186	31.603	0.948
xgBoost	7.434	0.100	11.230	0.995	15.317	0.167	26.521	0.964

All ensemble models model showed higher prediction capability on the test dataset compared to the base model (CART and SVM), as listed in **Table 5.2**. The evaluation of the performance of the selected model showed a very small difference between the experimental shear capacity and the predictions of the proposed xgBoost model in the testing phases as indicated by the RMSE of 26.522 kN for the test dataset. For the GBR

model, this value was 31.603 kN. The RMSE for the other models on the test dataset ranged between 41.848 kN to 57.416 kN. A similar trend was observed for other performance indices, as listed in **Table 5.2**. This observation illustrates the excellent prediction capacity of the proposed xgBoost model among all models, as listed in **Table 5.2**. Compared to all models, the CART model revealed the smallest performance with the maximum root mean square error and least R^2 on both train and test dataset, as presented in **Table 5.2**.

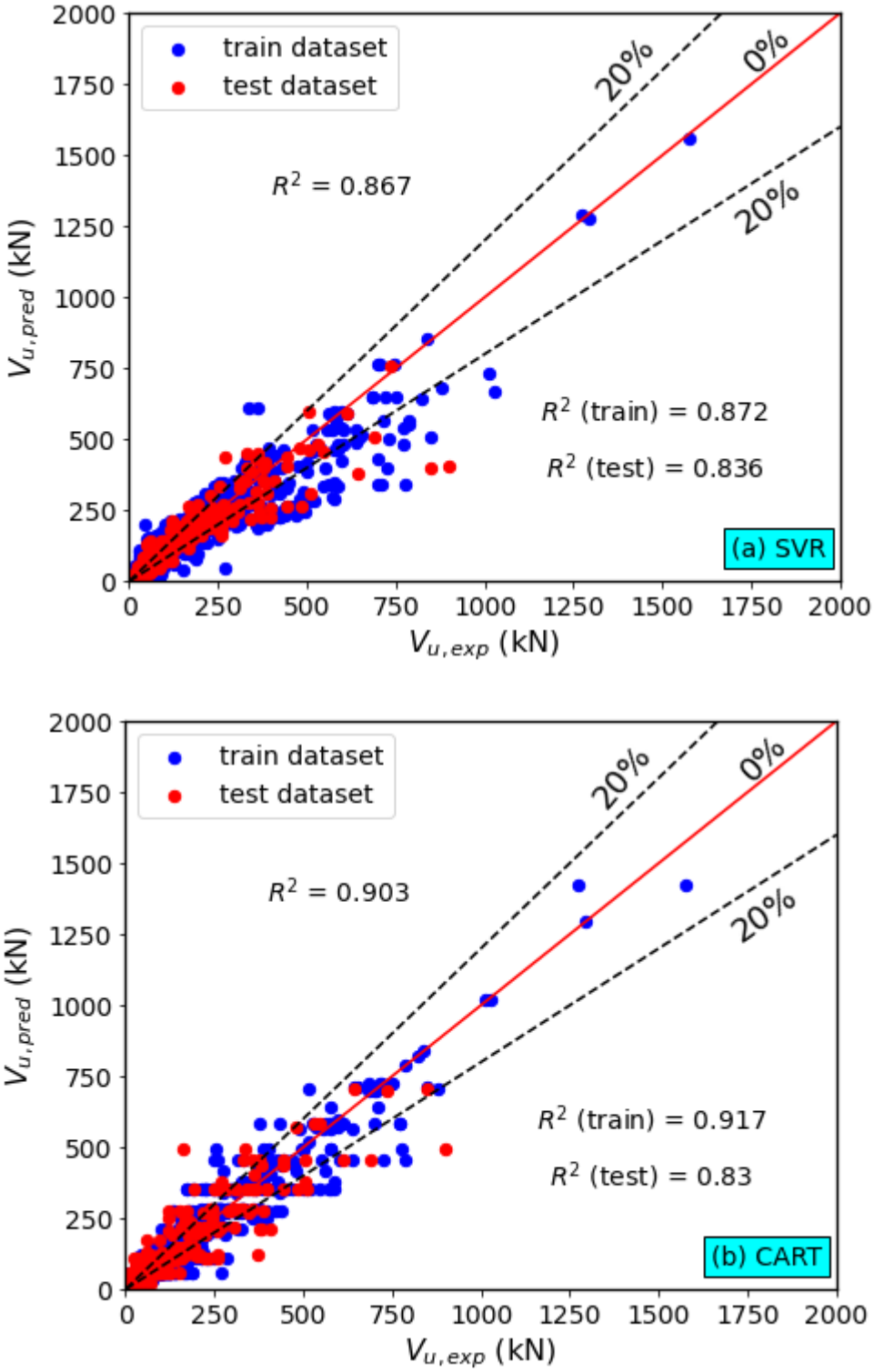

Figure 5.1: Comparisons of shear capacity predictions provided by the single ML models to the experimental shear capacity for RC beams without stirrup.

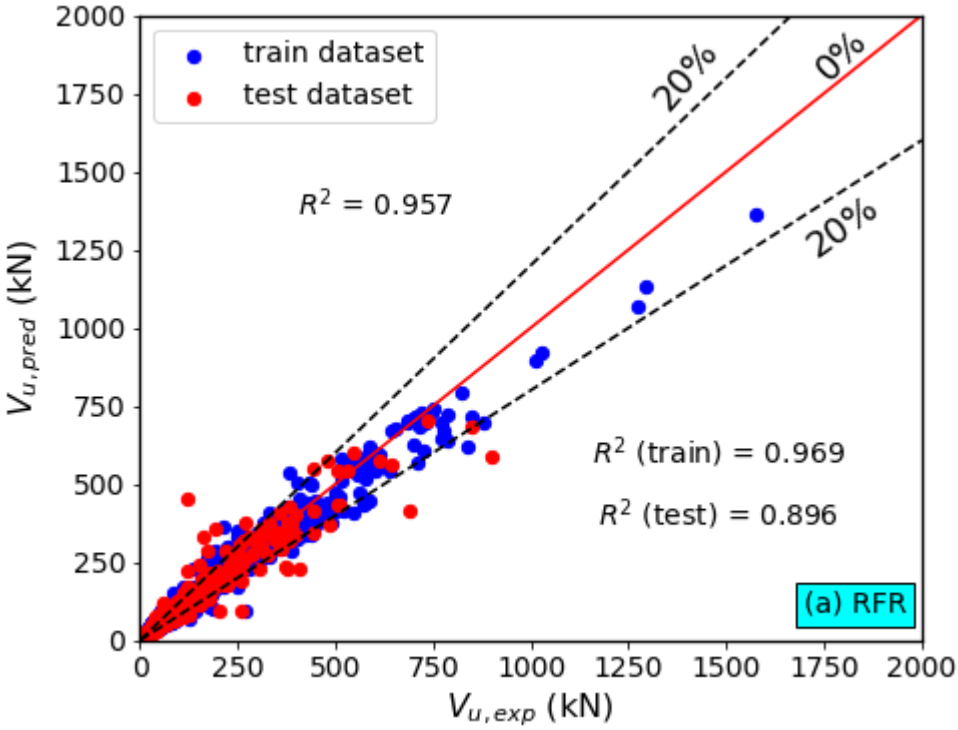
train dataset
test dataset
R^2 = 0.957
R^2 (train) = 0.969
R^2 (test) = 0.896
20%
0%
20%
(a) RFR
$V_{u,pred}$ (kN)
$V_{u,exp}$ (kN)
0
250
500
750
1000
1250
1500
1750
2000

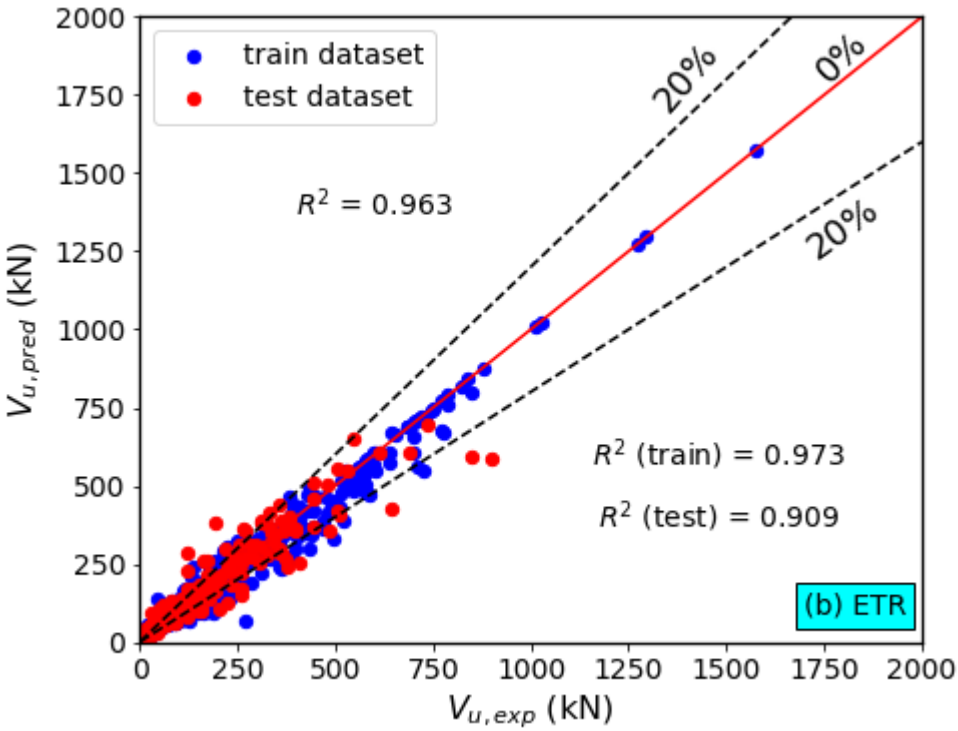
train dataset
test dataset
R^2 = 0.963
R^2 (train) = 0.973
R^2 (test) = 0.909
20%
0%
20%
(b) ETR
$V_{u,pred}$ (kN)
$V_{u,exp}$ (kN)
0
250
500
750
1000
1250
1500
1750
2000

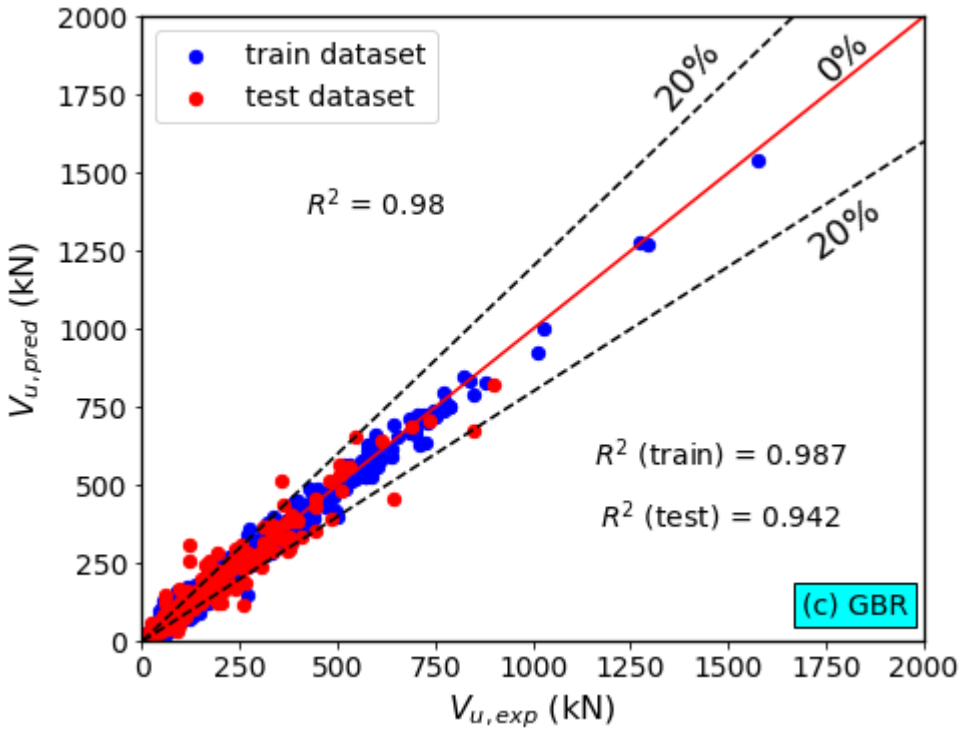

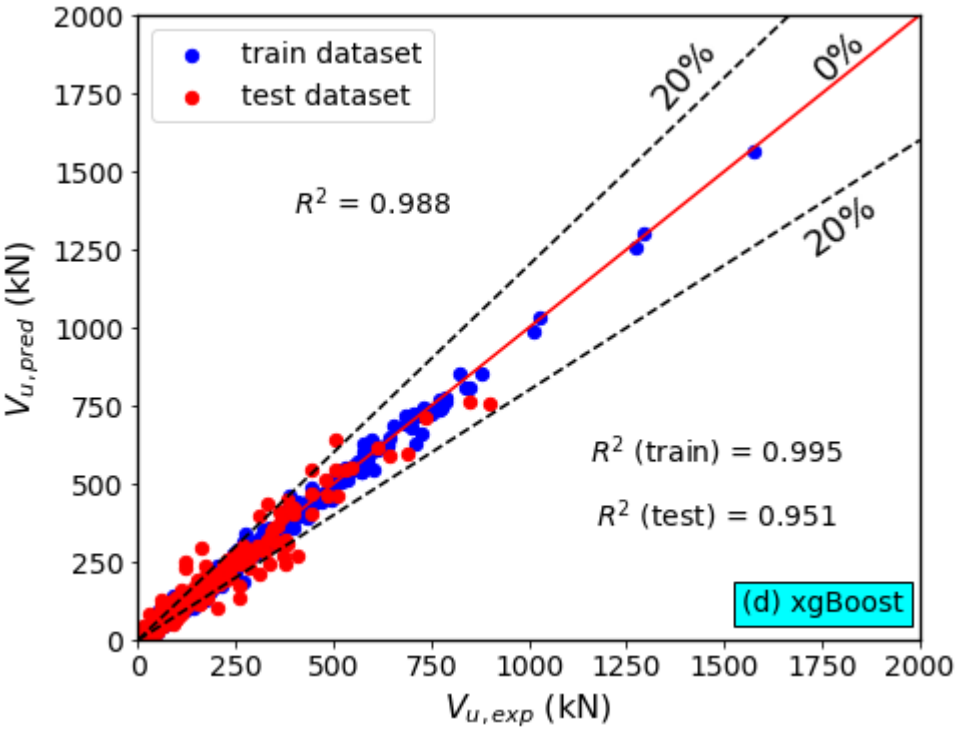

Figure 5.2: Comparisons of shear capacity predictions provided by the ensemble ML models to the experimental shear capacity for RC beams without stirrup.

Figures 5.1a–5.1b and Figures 5.2a–5.2d compare the shear capacity predicted by the ML models against the corresponding experimental values. As can be seen in these figures, the predictions provided by most of the models are in excellent agreement with the experimental values. It can also be observed from the same figures that the xgBoost model provided the best prediction for the load capacity of the beams, with the highest correlation between the experimental and predicted shear capacity for both the training and test datasets. A great correlation exists among the experimental and predicted shear capacities based on the xgBoost model as evidenced by the value of R^2 ($R^2 = 0.99$), as shown in **Fig. 5.2d** and **Table 5.2**.

Figures 5.3a and **5.3f** further compare the prediction capability of the models in terms of the residuals of the predicted shear capacity of the beams, which is the difference between the predicted shear capacity and the corresponding experimental value on the normalized training and test datasets. The figures also provide the correlation coefficient for both the training and test datasets. The residuals for all models are distributed around zero, as can be seen in **Figs. 5.3a–5.3f**. In addition, the proposed models generally resulted in a good correlation between the predicted and experimental load capaciies as can be evidenced from the values of coefficient of determination, as can be seen in **Figs. 5.3a–5.3f**. Compared to all models, xgBoost model showed the strongest correlation between the experimental shear capacity and its predicted value, as can be observed in **Fig. 5.3f**.

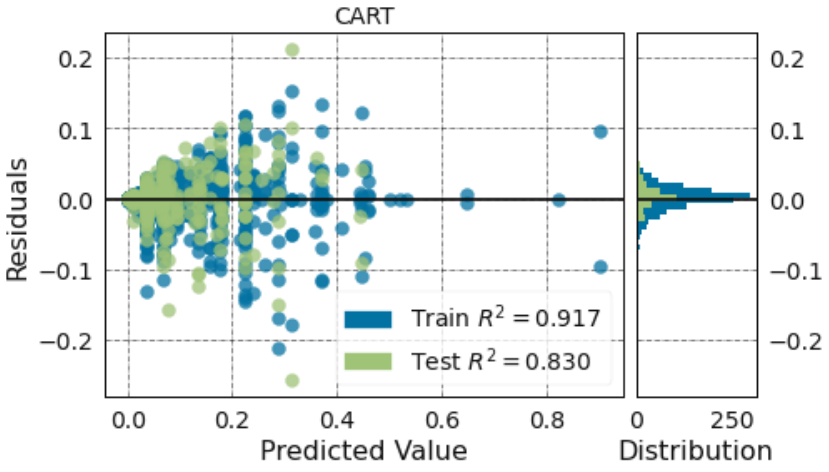
CART
Residuals
Predicted Value
Distribution
Train $R^2 = 0.917$
Test $R^2 = 0.830$

(a)

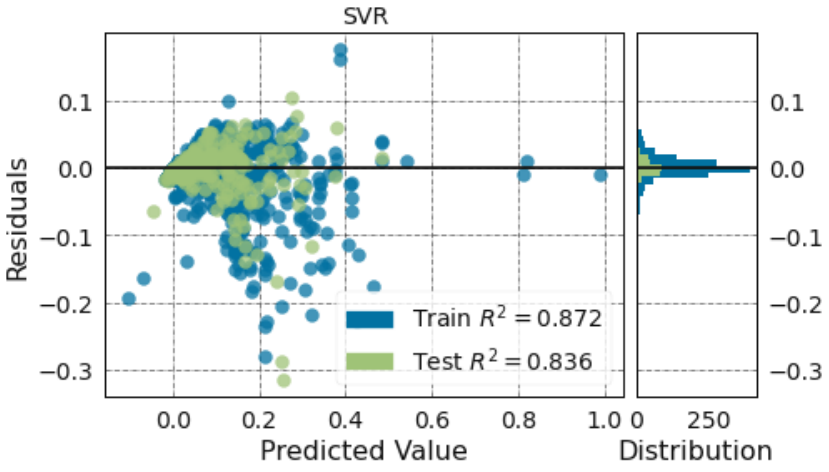
SVR
Residuals
Predicted Value
Distribution
Train $R^2 = 0.872$
Test $R^2 = 0.836$

(b)

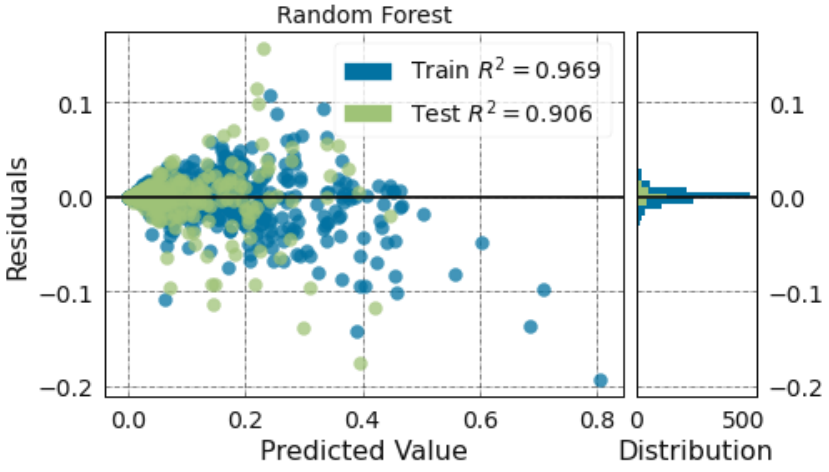
Random Forest
Residuals
Predicted Value
Distribution
Train $R^2 = 0.969$
Test $R^2 = 0.906$

(c)

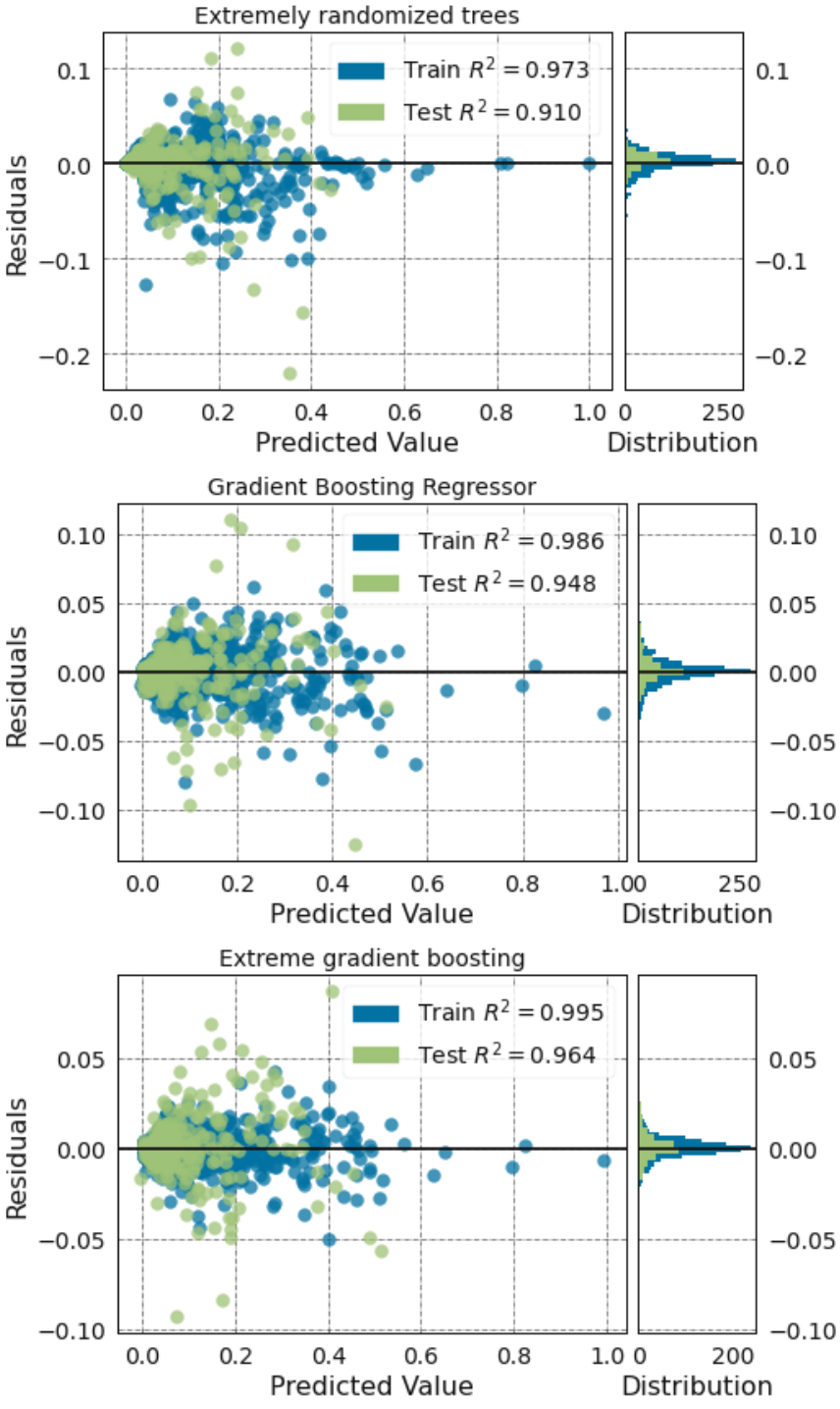

Figure 5.3: Residual plots for RC beams without stirrup.

5.1.1 Comparison with existing design guide line for RC beams without stirrup

The accuracy of the proposed ML model; particularly, xgBoost model is compared with that of the ACI 318 equation [55] and Eurocode 2. According to ACI 318 [55] and Eurocode 2, the shear capacity (V_n) of RC beam is evaluated as a simple superposition of the capacity provided by concrete (V_c) and transverse reinforcement (V_s).

$$V_n = V_c + V_s \quad \textbf{(35)}$$

Thus, for RC beams without stirrups, the nominal shear capacity (V_n) is given by the shear capacity provided by concrete (V_c). It is determined by equation (2) and equation (4) for AC1 318 and EC-2 respectively.

Table 5.3: Descriptive statics for V_{pred}/V_{exp} for RC beams without stirrup

Model	**mean**	**std**	**min**	**25%**	**50%**	**75%**	**max**
ACI-318	1.028372	0.231053	0.321645	0.938936	1.000643	1.07397	4.32554
EC-2	0.630559	0.344747	0.061932	0.41232	0.603127	0.773621	2.679892
xgBoost	0.526909	0.220215	0.055173	0.364288	0.561778	0.676812	1.331731

std: standard deviation, min: minimum, max: maximum

Figure 5.4 compares the predictive performance of the proposed xgBoost model with that of the ACI 318 equation [55] and Eurocode 2. As can be observed from this figure, the ACI and Eurocode 2 equation is inaccurate in predicting the shear capacity of the beams, as opposed to the proposed model that showed high accuracy in predicting the shear capacity of the beam. It can also be observed in **Fig. 5.4** that the ACI 318 and Eurocode 2 provision significantly underestimates the shear capacity for most of the beams.

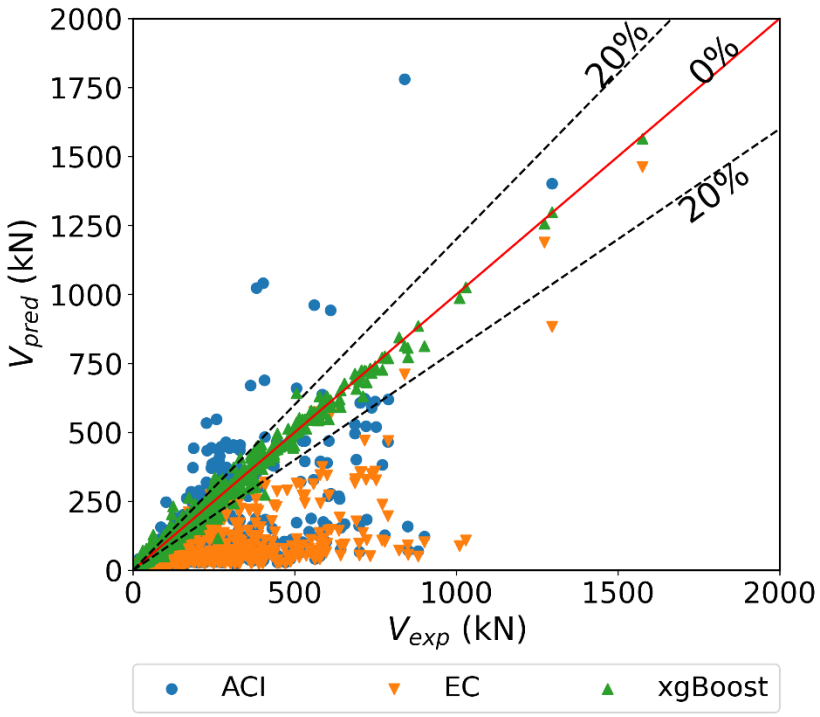

Figure 5.4: Predictions of ACI and proposed model for RC beams without stirrup.

Furthermore, the histogram in **Figures. 5.5a –5.5c** show the distribution of the predicted to experimental shear capacity ratio using the proposed xgBoost model, ACI 318 code equation and Eurocode 2. The proposed xgBoost model resulted in the most accurate and stable predictions, as can be seen in **Figures. 5.5a – 5.5c and table 5.3.** The average (μ) of the predicted to experimental shear capacity ratio was 1.03 for the proposed xgBoost model compared with an average of 0.63 and 0.53 for ACI 318 code equation and Eurocode 2 equation respectively. Furthermore, the standard deviation (σ) of 0.23 for proposed model and 0.36 and 0.22 for the ACI 318 code equation and EC-2 respectively.

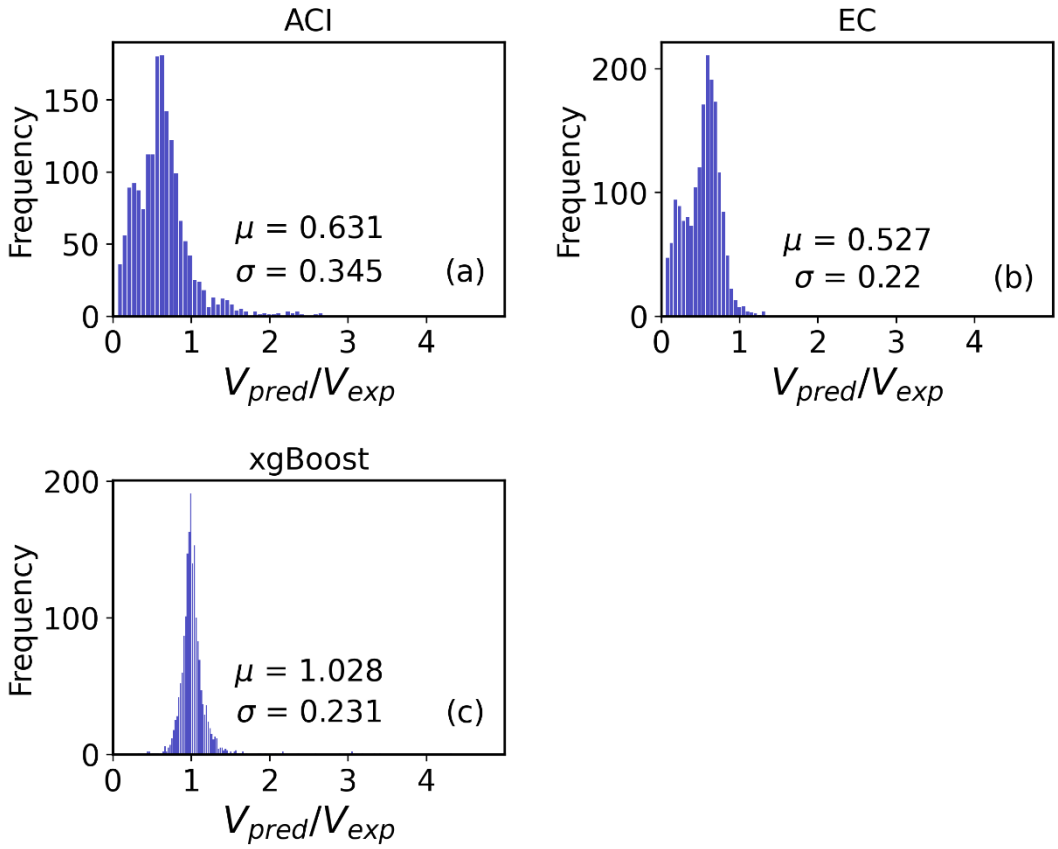

Figure 5.5: Histogram of predicted to experimental shear capacity ratio for RC beams without stirrup.

Table 5.4: Performance indices for xgBoost, ACI-318 and EC-2

Model	MAE	MAPE (%)	MSE	RMSE	R2
ACI	69.50109	44.24366	19111.12	138.243	0.149831
EC	76.73064	47.66816	19451.19	139.4675	0.183489
xgBoost	9.003983	11.2639	241.5076	15.54051	0.989865

Moreover, as showed in figure 5.13 and table 5.4 the root mean square error between experimental and predicted shear capacity is 15.54 for xgBoost model when it is 138.23

for ACI-318, and 139.47 for EC-2. The coefficient of determination (R^2) between experimental and predicted shear capacity is 99% for proposed xgBooost model, when it is 15% for ACI 138, and 18% Eurocode 2 equation. Compared to ACI-318 and EC-2 the proposed xgBoost model showed high performance with the lowest RMSE and highest correlation. Generally, it is concluded that the developed xgBoost model can reasonably estimate capacity of RC beams in shear.

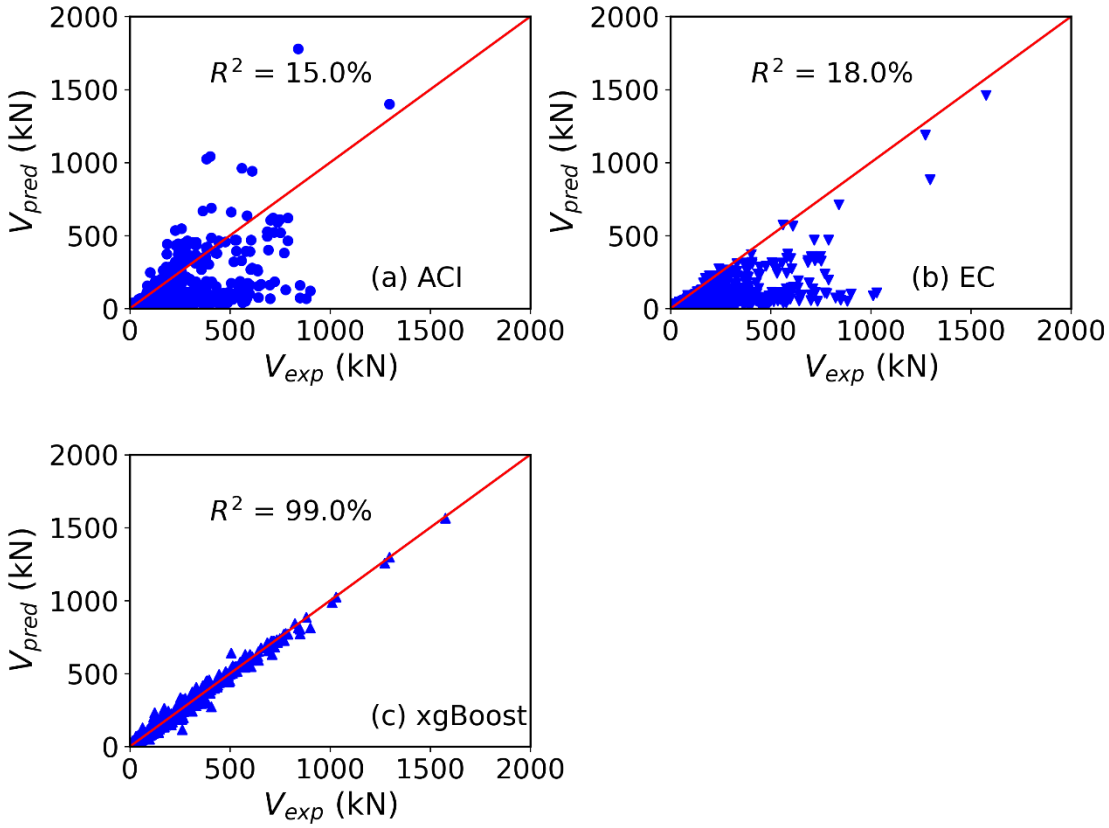

Figure 5.6 : Experimental versus predicted shear capacities for RC beams without stirrup based on the proposed xgBoost model and existing code equations.

5.2 RC beam with stirrup

In chapter four the dataset is prepared, the total of 348 RC beam with stirrup are included in the study. This section discusses the result from each models and comparative study

between proposed model, ACI 318 and EC-2. Similar to previous section, for RC beam with stirrup the hyperparameters for single and ensemble ML models are optimized by using 10-fold cross validation and presented in **Table 5.5**.

Table 5.5: Optimized hyperparameters of each models for RC beams with stirrup

Models	Optimized hyperparameters
SVR	Kernel type = radial basis function (rbf), ε = 0.1, C = 195
CART	Maximum depth = 8, maximum features = 5, minimum sample leaf = 1, minimum sample split = 2
RFR	Number of estimators = 34, depth_max = 15, features_max = 5, minimum sample split = 2
ERT	Number of estimators = 29, depth_max = 10, maximum features = 7
GTBR	Number of estimators = 55, depth_max = 8, rate of learn = 0.3, subs ample = 0.3, maximum features = 6
xgBoost	Number of estimators = 165, maximum depth = 9, rate of learn = 0.12, subsample = 0.4

Figure 5.7 shows a 7 × 7 matrix in which the diagonal of the matrix shows the histogram for the distribution of each variable, whereas the lower and upper triangular matrices show the scatter plot and Pearson correlation coefficient (r) between the input variables, respectively. As can be observed in this figure, there is complex relationship between the parameters that influence shear capacity of RC beam.

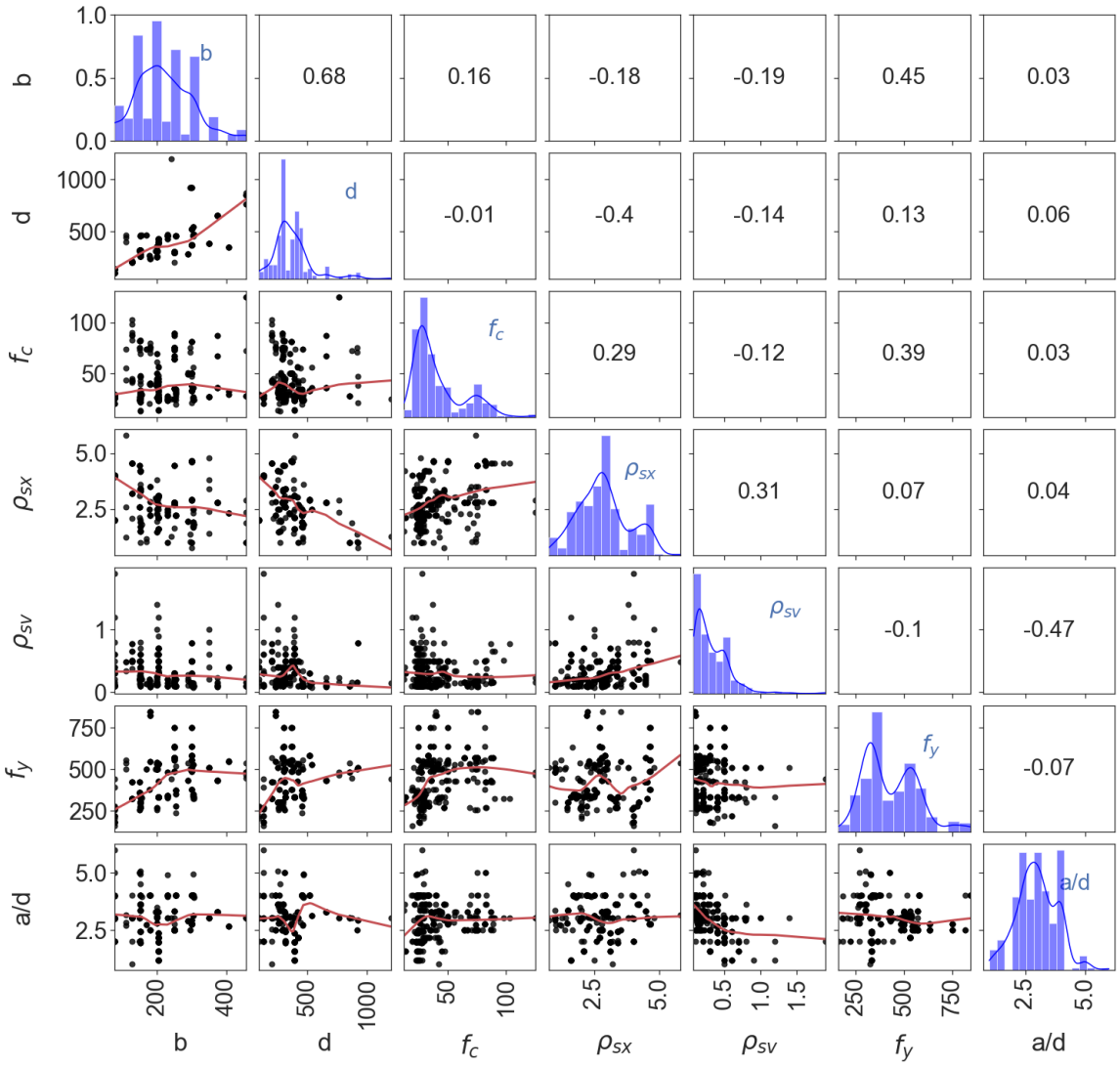

Figure 5.7: Properties of dataset for RC beams with stirrups.

The total of 348 RC beams with stirrup are included in dataset, the dataset is randomly split into 80% and 20% of test and train dataset respectively. The performance indices regarding to the test and train dataset for each model (SVM, CART, RFR, ERT, GBR, xgBoost) are evaluated and listed in **Table 5.6**. Compering the base models and ensemble models, the ensemble models showed the highest performance to predict the shear capacity of RC beam with RMSE of between 42.873 kN and 35.743 kN for test dataset, when it is

range between 112.416 kN and 55.851 kN for single or base models. From all models the selected model showed a very small difference between the experimental shear capacity and the predictions of the proposed xgBoost model in the testing phases as indicated by the RMSE and R^2 of 35.743 kN and 0.995 respectively. A similar trend was observed for other performance indices, as listed in **Table 5.6**. This observation illustrates the superior prediction capability of the proposed xgBoost model among all models, as listed in **Table 5.6**. Compared to all models, the SVR model showed the lowest performance with the highest root mean square error and least R^2 on both the test and train dataset, as presented in **Table 5.6**.

Table 5.6: Performance indices for RC beams with stirrup

Model	Training dataset				Test dataset			
	MAE	MAPE	RMSE	R2	MAE	MAPE	RMSE	R2
SVR	93.556	51.295	122.362	0.798	81.882	70.038	112.416	0.868
CART	19.083	7.628	32.958	0.985	37.435	15.471	55.851	0.967
RFR	17.800	6.252	32.836	0.985	29.044	12.509	42.873	0.981
ETR	10.897	4.167	19.794	0.995	26.710	11.447	38.341	0.985
GBR	12.219	6.055	19.825	0.995	25.058	17.046	32.698	0.989
xgBoost	6.425	2.513	11.823	0.998	27.036	14.009	35.743	0.987

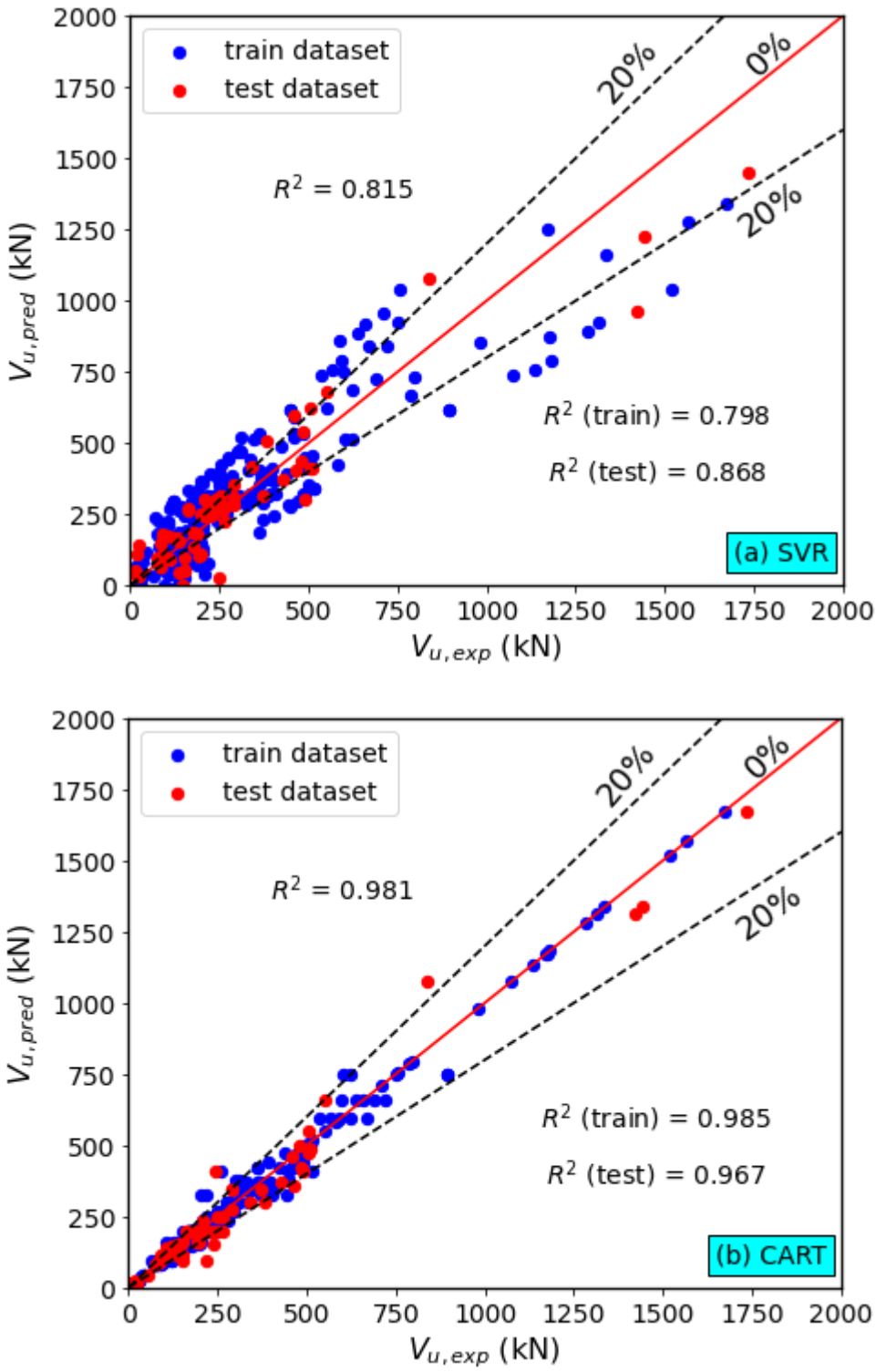

Figure 5.8: Comparisons of shear capacity predictions provided by single ML models to the experimental shear capacity for RC beam with stirrup.

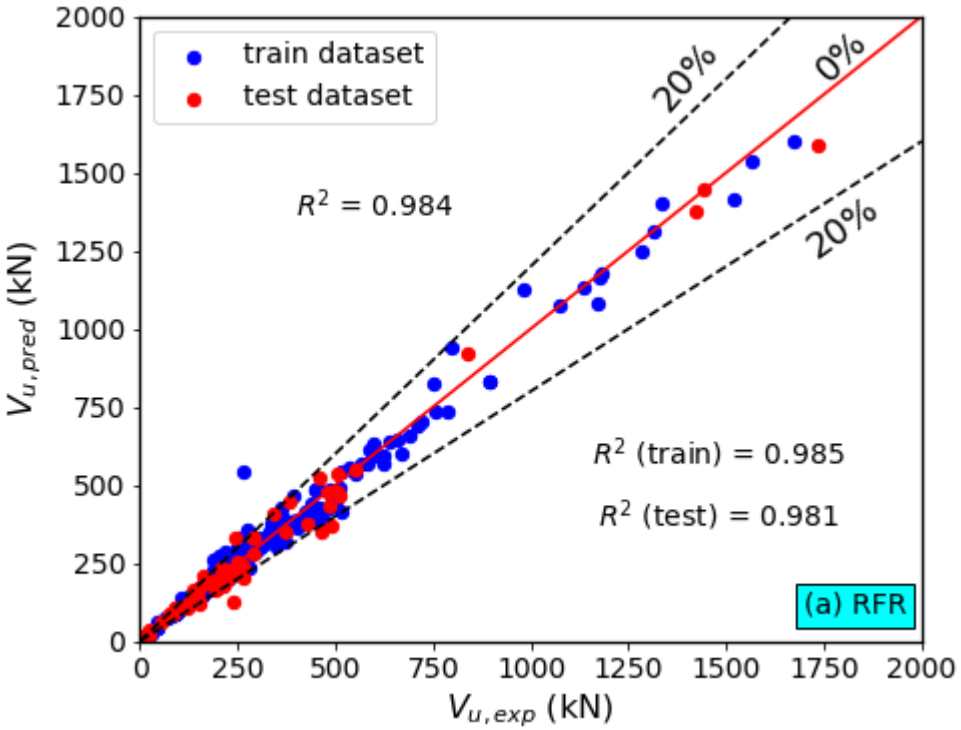
train dataset
test dataset
R^2 = 0.984
R^2 (train) = 0.985
R^2 (test) = 0.981
20%
0%
20%
(a) RFR
$V_{u,pred}$ (kN)
$V_{u,exp}$ (kN)
0
250
500
750
1000
1250
1500
1750
2000

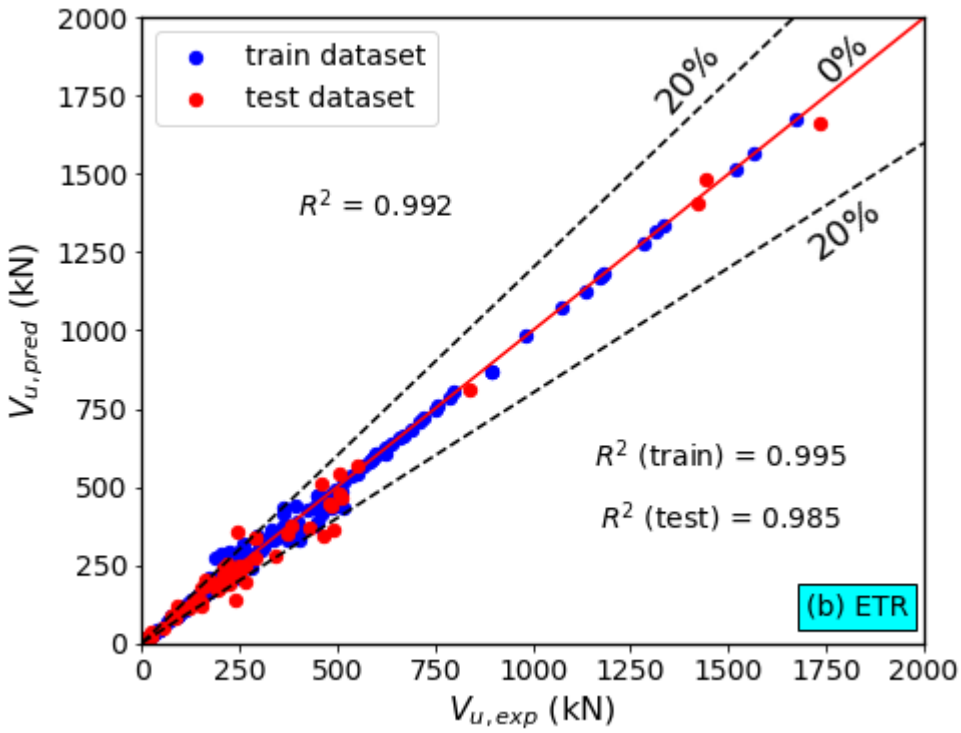
train dataset
test dataset
R^2 = 0.992
R^2 (train) = 0.995
R^2 (test) = 0.985
20%
0%
20%
(b) ETR
$V_{u,pred}$ (kN)
$V_{u,exp}$ (kN)
0
250
500
750
1000
1250
1500
1750
2000

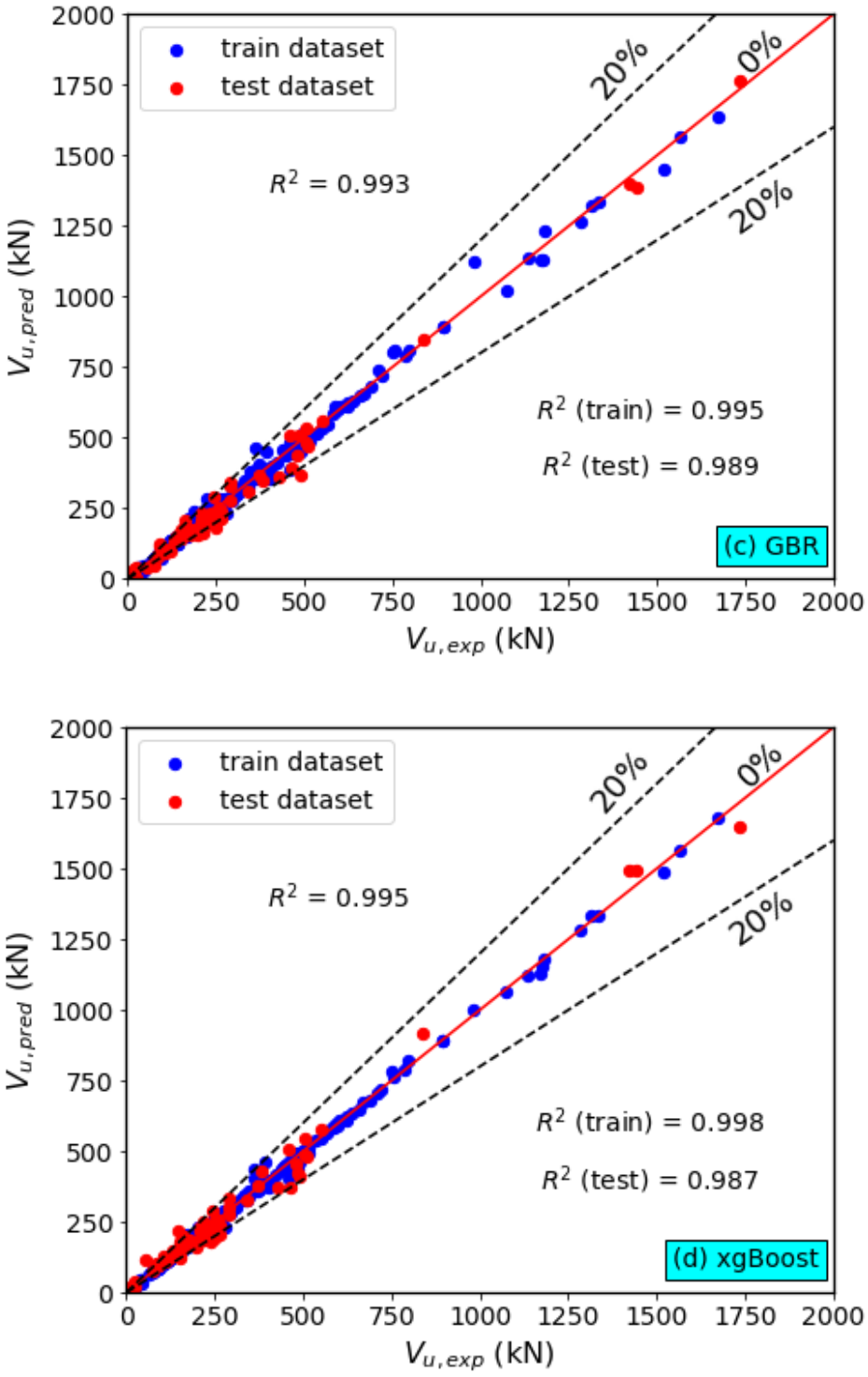

Figure 5.9: Comparisons of shear capacity predictions provided by ensemble ML models to the experimental shear capacity for RC beam with stirrup.

For RC beams with stirrup **Figures 5.9a–5.9b** compare the shear capacity predicted by single ML models and the corresponding experimental values. From single model CART models showed highest shear capacity predictions with R^2 of 0.981. However **Figures 5.10a–5.10d** compare the shear capacity predicted by ensemble ML models and corresponding experimental values. As can be observed in these figures, the predictions provided by ensemble ML models are in excellent agreement with the experimental values. It can also be observed from the same figures that the xgBoost model provided the best prediction for the shear capacity of the beams, with the highest correlation between the experimental and predicted shear capacity for both the test and train datasets. A solid correlation exists between the experimental and predicted shear capacities based on the xgBoost model as evidenced by the value of R^2 ($R^2 = 0.995$), as shown in **Figure. 5.10d** and **Table 5.6**.

5.2.1 Comparison with existing design guide line for RC beams with stirrup

The performance of the proposed xgBoost model ML model is compared with that of the ACI 318 equation [55] Eurocode equation. According to ACI 318 [55] and Eurocode 2 design guideline equation, the nominal shear capacity (V_n) of RC beam with stirrups is evaluated as a simple superposition of the capacity provided by concrete (V_c) and transverse reinforcement (V_s). It is evaluated by equation (1) and equation (7) respectively.

Table 5.7: Descriptive statics for V_{pred}/V_{exp} for RC beams with stirrup

Model	**mean**	**std**	**min**	**25%**	**50%**	**75%**	**max**
ACI-318	0.743987	0.446266	0.260748	0.583917	0.701994	0.807901	5.05479
EC-2	0.274128	0.258981	0.043825	0.173477	0.224379	0.305725	2.898384
xgBoost	1.009169	0.101862	0.743393	0.979759	1.000558	1.021289	2.065771

std: standard deviation, min: minimum, max: maximum

Figure 5.11 compares the predictive performance of the proposed xgBoost model with that of the ACI 318 equation [55] and Eurocode 2. As can be observed from this figure, the ACI equation and EC-2 equation are inaccurate in predicting the shear capacity of the RC beam with stirrup, as opposed to the proposed model that showed high accuracy in predicting the shear capacity of the beam. It can also be observed in **Fig. 5.11** that the ACI 318 and Eurocode 2 provision significantly underestimates the shear capacity for most of the beams.

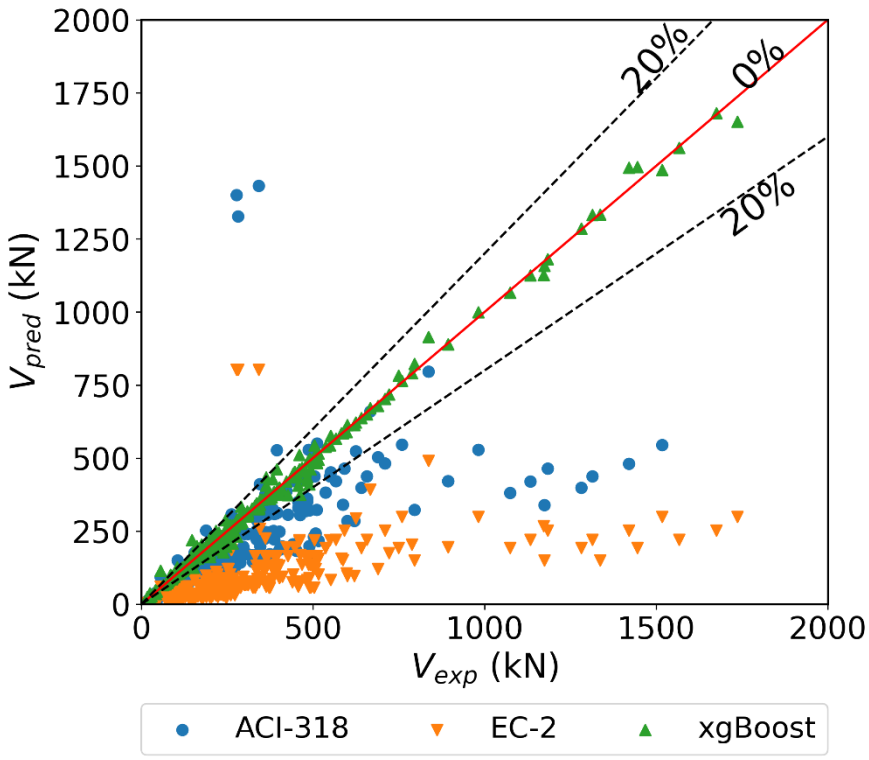

Figure 5.10: Predictions of ACI, Eurocode and proposed model for RC beams with stirrup.

Moreover, the histogram in **Figures. 5.12a –5.12c** show the distribution of the predicted to experimental shear capacity ratio using the proposed xgBoost model, ACI 318 code equation and Eurocode 2. The proposed xgBoost model resulted in the most accurate and stable predictions, as can be seen in **Figures. 5.12a – 5.12c and table 5.7.** The average (μ) of the predicted to experimental shear capacity ratio was 1.01 for the proposed xgBoost model compared with an average of 0.74 and 0.27 for ACI 318 code equation and Eurocode 2 equation respectively. Furthermore, the standard deviation (σ) of 0.102 for proposed model and 0.45 and 0.26 for the ACI 318 and EC-2 code equation respectively.

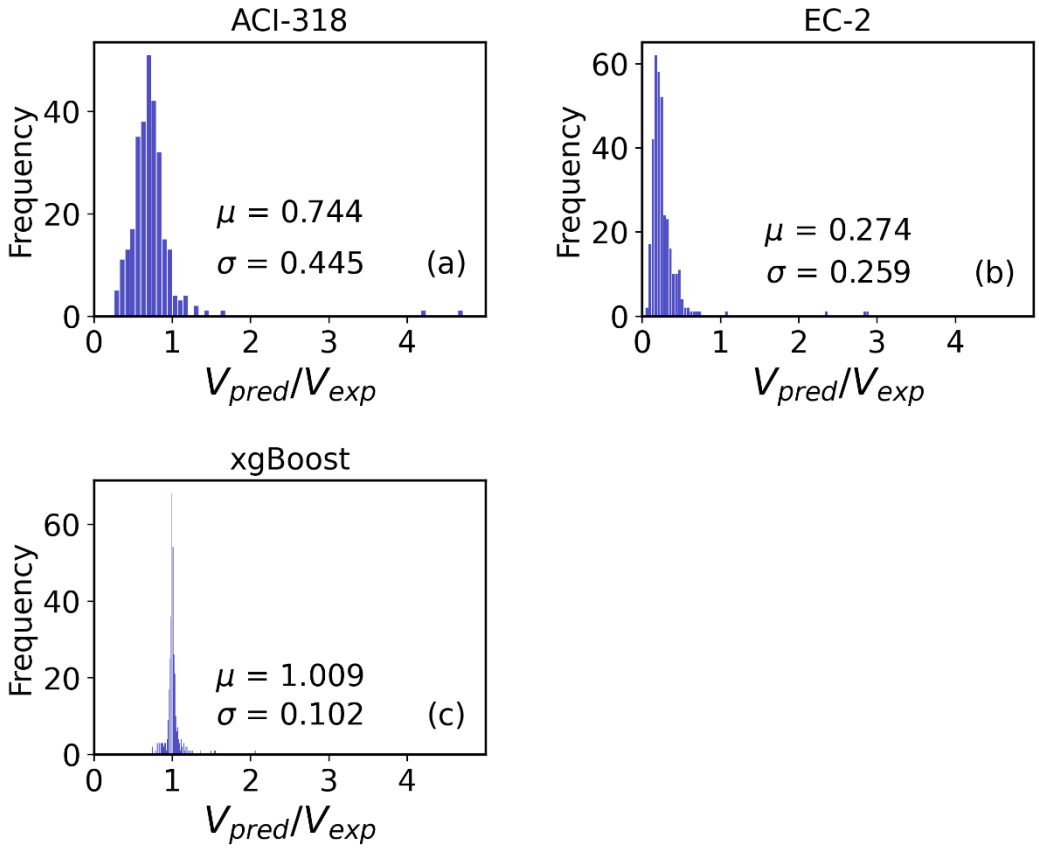

Figure 5.11: Histogram of predicted to experimental shear capacity for RC beams with stirrup

Table 5.8 : Performance indices for xgBoost, ACI-318 and EC-2

Model	MAE	MAPE (%)	MSE	RMSE
ACI-318	111.6445	35.07028	44480.63	210.9043
EC-2	229.2035	75.60847	104698.1	323.5708
xgBoost	10.5715	4.825852	368.6531	19.20034

Furthermore, as showed in figure 5.13 and table 5.8 the root mean square error between experimental and predicted shear capacity is 19.20 for xgBoost model when it is 210.90

for ACI-318, and 323.57 for EC-2. The value of R^2 between experimental and predicted shear capacity is 99.5% for proposed xgBooost model. Compared to ACI-318 and EC-2 the proposed xgBoost model showed high performance with the lowest RMSE and highest R^2. Generally, it can be concluded that the proposed xgBoost model can accurately predict capacity of RC beams in shear.

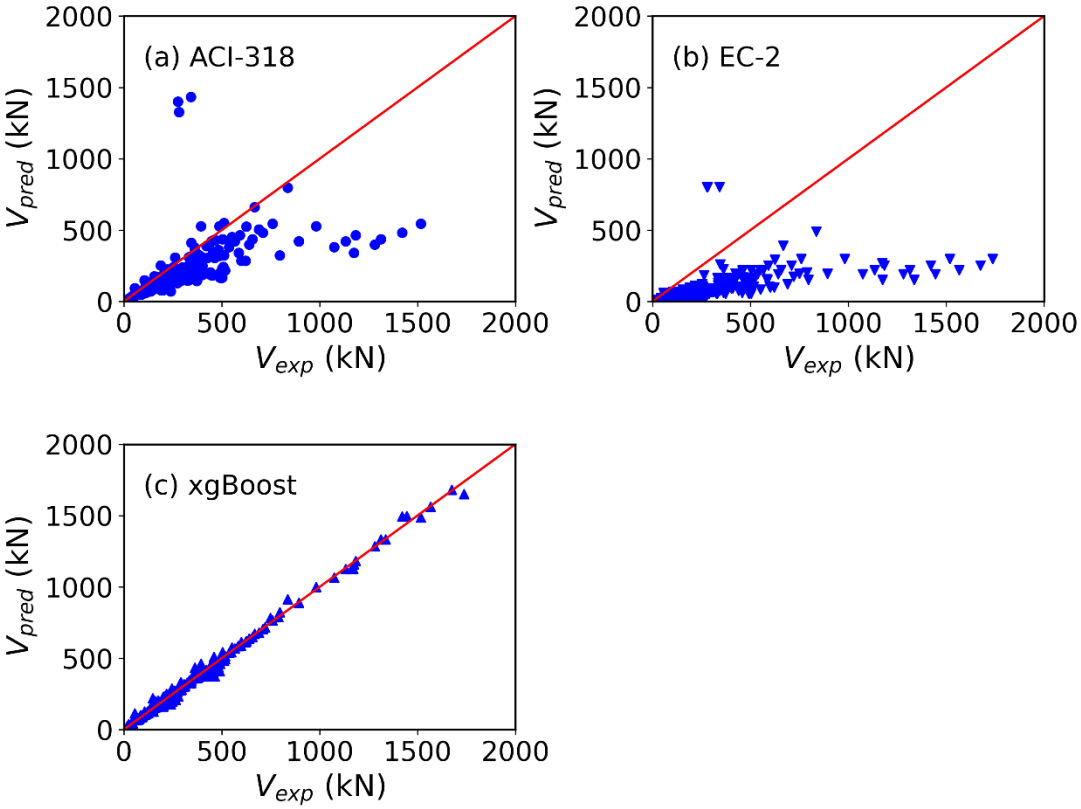

Figure 5.12 : Experimental versus predicted shear capacities for RC beams with stirrup based on the proposed xgBoost model and existing code equations.

5.3 Deployment of the ML model to a web-based application

The developed xgBoost model is deployed to a user-friendly web-based application. The deployed model can be accessed at: https://shearcapaity.herokuapp.com/. Alternatively, it can be accessed via the following QR code.

The deployed model is under development. It can be used for the reliable and accurate shear design of RC beams. Particularly, it is of great interest to practitioners and designers as it is user-friendly and superior in terms of its prediction capability compared to other available models and code equations. The developed web-based application does not require knowledge of the machine learning algorithms. This makes it very attractive to the practitioners and researchers in the field of civil engineering. It can also be used for the teaching purpose as a quick and accurate determination of the capacity of RC beams in shear. The screenshot of the deployed model is shown below.

As can be seen in the screen shoot above, the input parameters are listed on the left hand side. The user should define the input variables by scrolling under each input parameter. Once the definition for the input variables are complete, the summary of the values of the input parameters can be seen on the right hand side under “user defined variables”. The capacity of RC beams in shear based on the defined variables can then be read on the same screen. The developed application can be used in any device including mobile phones, tablets, and computers. Hence, it is user-friendly to be used by any interested individual without prior knowledge in the machine learning algorithms and also the theory behind the shear mechanisms.

CHAPTER 6 CONCLUSIONS AND RECOMMENDATIONS

6.1 Conclusions

Despite several experimental studies aimed to understand the structural response of reinforced concrete (RC) beams, accurate prediction of their shear capacity remains a challenge. To this end, data-driven ensemble ML-based models to predict the shear capacity of RC beams are presented in this paper. This study has shown that the ML model can be used as effective tools to predict the shear capacity of RC beam. The proposed models account for several input parameters that characterize the beam geometry, concrete strength, and flexural reinforcement and transversal reinforcement. The prediction capability of the ML-based models is compared with that of the ACI 318 equation and Eurocode 2.

- The developed ML-based models are shown to be effective in predicting the shear capacity of RC beams. Generally, all models showed good prediction capability for RC beams with/withour stirrups.
- The ensemble models provided higher accuracy compared to the single models.
- Among ML models, xgBoost showed the highest prediction capability with the lowest RMSE and highest correlation for the test dataset. The experimental shear capacity and predicted values based on the xgBoost model showed the strongest correlation with a coefficient of determination (R^2) of 0.99 for RC beam without stirrup and 0.995 for RC beam with stirrups.
- The comparisons of the proposed models with the existing code equation confirmed the superiority of the xgBoost model. The ACI 318 and Eurocode 2

provision significantly underestimates the shear capacity of RC beams with and without stirrups.

- The findings of this study showed the successful implementation of machine learning techniques to predict the shear capacity of shear-critical RC beams.
- With an aim to develop an accurate and user-friendly shear design model, the developed xgBoost model is deployed to a user-friendly web-based application: https://shearcapaity.herokuapp.com/.

Future research is recommended to incorporate reliability study and other types of reinforcement including fiber reinforced polymer (FRP) reinforcement. Moreover, it is recommended to investigate the flexural response of RC beams using data-driven ML-based models.

REFERENCES

[1] Baghi H, Barros JAO. New Approach to Predict Shear Capacity of Reinforced Concrete Beams Strengthened with Near-Surface-Mounted Technique. ACI Struct J 2016;114. https://doi.org/10.14359/51689433.

[2] Minelli F, Vecchio FJ. Compression Field Modeling of Fiber-Reinforced Concrete Members Under Shear Loading. ACI Struct J 2006;103:244–52.

[3] ACI Committee 318. Building code requirements for structural concrete (ACI 318-14). American Concrete Institute, Farmington Hills, MI, USA.; 2014.

[4] BS EN 1992-1-1. Eurocode 2: Design of concrete structures - Part 1-1 : General rules and rules for buildings. vol. 1. Brussels, Belgium: European Committee for Standardization; 2004.

[5] Salehi H, Burgueño R. Emerging artificial intelligence methods in structural engineering. Eng Struct 2018;171:170–89. https://doi.org/10.1016/j.engstruct.2018.05.084.

[6] Demir F. Prediction of elastic modulus of normal and high strength concrete by artificial neural networks. Constr Build Mater 2008;22:1428–35. https://doi.org/10.1016/j.conbuildmat.2007.04.004.

[7] Perera R, Ruiz A, Manzano C. An evolutionary multiobjective framework for structural damage localization and quantification. Eng Struct 2007;29:2540–50. https://doi.org/10.1016/j.engstruct.2007.01.003.

[8] Lee S. Prediction of concrete strength using artificial neural networks. Eng Struct 2003;25:849–57. https://doi.org/10.1016/S0141-0296(03)00004-X.

[9] Chaabene W Ben, Flah M, Nehdi M. Machine learning prediction of mechanical

properties of concrete: Critical review. Constr Build Mater 2020;260:119889. https://doi.org/10.1016/j.conbuildmat.2020.119889.

[10] Trocoli A, Dantas A, Leite MB, Nagahama KDJ. Prediction of compressive strength of concrete containing construction and demolition waste using artificial neural networks. Constr Build Mater 2013;38:717–22. https://doi.org/10.1016/j.conbuildmat.2012.09.026.

[11] Inel M. Modeling ultimate deformation capacity of RC columns using artificial neural networks. Eng Struct 2007;29:329–35. https://doi.org/10.1016/j.engstruct.2006.05.001.

[12] Jiang K, Han Q, Bai Y, Du X. Data-driven ultimate conditions prediction and stress-strain model for FRP-confined concrete. Compos Struct 2020;242:112094. https://doi.org/10.1016/j.compstruct.2020.112094.

[13] Naderpour H, Kheyroddin A, Amiri GG. Prediction of FRP-confined compressive strength of concrete using artificial neural networks. Compos Struct 2010;92:2817–29. https://doi.org/10.1016/j.compstruct.2010.04.008.

[14] Jalal M, Ramezanianpour AA. Strength enhancement modeling of concrete cylinders confined with CFRP composites using artificial neural networks. Compos Part B Eng 2012;43:2990–3000. https://doi.org/10.1016/j.compositesb.2012.05.044.

[15] Elsanadedy HM, Al-Salloum YA, Abbas H, Alsayed SH. Prediction of strength parameters of FRP-confined concrete. Compos Part B Eng 2012;43:228–39. https://doi.org/10.1016/j.compositesb.2011.08.043.

[16] Flood I. Towards the next generation of artificial neural networks for civil engineering. Adv Eng Informatics 2008;22:4–14.

https://doi.org/10.1016/j.aei.2007.07.001.

[17] Mangalathu S, Jang H, Hwang S-H, Jeon J-S. Data-driven machine-learning-based seismic failure mode identification of reinforced concrete shear walls. Eng Struct 2020;208:110331. https://doi.org/10.1016/j.engstruct.2020.110331.

[18] Keshtegar B, Nehdi ML, Trung N-T, Kolahchi R. Predicting load capacity of shear walls using SVR-RSM model. Appl Soft Comput 2021:107739. https://doi.org/10.1016/j.asoc.2021.107739.

[19] Hwang SH, Mangalathu S, Shin J, Jeon JS. Machine learning-based approaches for seismic demand and collapse of ductile reinforced concrete building frames. J Build Eng 2021;34. https://doi.org/10.1016/j.jobe.2020.101905.

[20] Mangalathu S, Hwang SH, Choi E, Jeon JS. Rapid seismic damage evaluation of bridge portfolios using machine learning techniques. Eng Struct 2019;201. https://doi.org/10.1016/j.engstruct.2019.109785.

[21] Mangalathu S, Sun H, Nweke CC, Yi Z, Burton H V. Classifying earthquake damage to buildings using machine learning. Earthq Spectra 2020;36:183–208. https://doi.org/10.1177/8755293019878137.

[22] Yan W, Deng L, Zhang F, Li T, Li S. Probabilistic machine learning approach to bridge fatigue failure analysis due to vehicular overloading. Eng Struct 2019;193:91–9. https://doi.org/10.1016/j.engstruct.2019.05.028.

[23] Weinstein JC, Sanayei M, Asce M, Brenner BR, Asce F. Bridge Damage Identification Using Artificial Neural Networks. J Bridg Eng 2018;23:04018084. https://doi.org/10.1061/(ASCE)BE.1943-5592.0001302.

[24] Fathalla E, Tanaka Y, Maekawa K. Remaining fatigue life assessment of in-service road bridge decks based upon arti fi cial neural networks. Eng Struct 2018;171:602–

16. https://doi.org/10.1016/j.engstruct.2018.05.122.

[25] Morfidis K, Kostinakis K. Approaches to the rapid seismic damage prediction of r/c buildings using artificial neural networks. Eng Struct 2018;165:120–41. https://doi.org/10.1016/j.engstruct.2018.03.028.

[26] Caglar N. Neural network based approach for determining the shear strength of circular reinforced concrete columns. Constr Build Mater 2009;23:3225–32. https://doi.org/10.1016/j.conbuildmat.2009.06.002.

[27] Jalal M, Arabali P, Grasley Z, Bullard JW, Jalal H. Behavior assessment, regression analysis and support vector machine (SVM) modeling of waste tire rubberized concrete. J Clean Prod 2020;273:122960. https://doi.org/10.1016/j.jclepro.2020.122960.

[28] Pal M, Deswal S. Support vector regression based shear strength modelling of deep beams. Comput Struct 2011;89:1430–9. https://doi.org/10.1016/j.compstruc.2011.03.005.

[29] Solhmirzaei R, Salehi H, Kodur V, Naser MZ. Machine learning framework for predicting failure mode and shear capacity of ultra high performance concrete beams. Eng Struct 2020;224:111221. https://doi.org/10.1016/j.engstruct.2020.111221.

[30] Tuv E. Ensemble learning. Stud Fuzziness Soft Comput 2006;207:187–204. https://doi.org/10.1007/978-3-540-35488-8_8.

[31] Breiman L. Bagging predictors. Mach Learn 1996;24:123–40. https://doi.org/10.3390/risks8030083.

[32] Wolpert D. Stacked Generalization. Neural Networks 1992;5:241–59.

[33] Zhou H, Huang G Bin, Lin Z, Wang H, Soh YC. Stacked extreme learning

machines. IEEE Trans Cybern 2015;45:2013–25. https://doi.org/10.1109/TCYB.2014.2363492.

[34] Sanad A, Saka MP. Prediction of ultimate shear strenggth of reinforced concrete deep beams using Neural Networks. J Struct Eng 2001;127:818–28.

[35] Cladera A, Mari AR. Shear design procedure for reinforced normal and high-strength concrete beams using artificial neural networks. Part I: beams without stirrups. Eng Struct 2004;26:917–26. https://doi.org/10.1016/j.engstruct.2004.02.010.

[36] Chou J, Ngo N, Pham A. Shear Strength Prediction in Reinforced Concrete Deep Beams Using Nature-Inspired Metaheuristic Support Vector Regression 2012;30:1–9. https://doi.org/10.1061/(ASCE)CP.1943-5487.0000466.

[37] Naderpour H, Mirrashid M. Shear strength prediction of RC beams using adaptive neuro-fuzzy inference system. Sci Iran 2020;27:657–70. https://doi.org/10.24200/sci.2018.50308.1624.

[38] Chou JS, Pham TPT, Nguyen TK, Pham AD, Ngo NT. Shear strength prediction of reinforced concrete beams by baseline, ensemble, and hybrid machine learning models. Soft Comput 2020;24:3393–411. https://doi.org/10.1007/s00500-019-04103-2.

[39] Cladera A, Mari AR. Shear design procedure for reinforced normal and high-strength concrete beams using artificial neural networks. Part II: beams with stirrups. Eng Struct 2004;26:927–36. https://doi.org/10.1016/j.engstruct.2004.02.011.

[40] Friedman JH, Hastie T, Tibshirani R. The Elements of Statistical Learning. 2001. https://doi.org/10.1111/j.1467-985x.2004.298_11.x.

[41] Collins MP, Bentz EC, Sherwood EG. Where is shear reinforcement required? Review of research results and design procedures. ACI Struct J 2008;105:590–600. https://doi.org/10.14359/19942.

[42] Zhang T, Visintin P, Oehlers DJ. Shear strength of RC beams with steel stirrups. J Struct Eng 2016;142:04015135. https://doi.org/10.1061/(ASCE)ST.1943-541X.0001404.

[43] Pathuri JR, Diaz M, Ph D, Montoya A, Ph D. Effect of longitudinal reinforcement strength on shear strength of reinforced concrete beams and slabs by Presented to the Graduate Faculty of The University of Texas at San Antonio in Partial Fulfillment of the Requirements for the Degree of . MASTER OF. 2017.

[44] Fernández Ruiz M, Muttoni A, Sagaseta J. Shear strength of concrete members without transverse reinforcement: A mechanical approach to consistently account for size and strain effects. Eng Struct 2015;99:360–72. https://doi.org/10.1016/j.engstruct.2015.05.007.

[45] El-Ariss B. Behavior of beams with dowel action. Eng Struct 2007;29:899–903. https://doi.org/10.1016/j.engstruct.2006.07.008.

[46] Ormberg G. Evaluating Shear Capacity of Concrete Members with Deficient Shear Reinforcement. 2010.

[47] ACI Committee 318. Building Code Requirements for Structural Concrete and commentary (ACI 318–14). Am Concr Institute, Farmingt Hills, MI 2011:524.

[48] Tompos EJ, Frosch RJ. Influence of beam size, longitudinal reinforcement, and stirrup effectiveness on concrete shear strength. ACI Struct J 2002;99:559–67.

[49] Bentz EC. Empirical modeling of reinforced concrete shear strength size effect for members without stirrups. ACI Struct J 2005;102:232–41.

https://doi.org/10.14359/14274.

[50] Zararis PD, Zararis IP. Shear Strength of Reinforced Concrete Beams under Uniformly Distributed Loads. ACI Struct J 2008;105:711–9.

[51] Hu B, Wu YF. Effect of shear span-to-depth ratio on shear strength components of RC beams. Eng Struct 2018;168:770–83. https://doi.org/10.1016/j.engstruct.2018.05.017.

[52] Collins MP, Bentz EC, Sherwood EG. Where is shear reinforcement require? Review of research results and design procedures. ACI Struct J 2009.

[53] Joint ACI-ASCE Committee 445. Recent approaches to shear design of structural concrete. J Struct Eng 1998;124:1374–417. https://doi.org/10.1061/(ASCE)0733-9445(1998)124:12(1375).

[54] Baghi H, Barros JAO. Design approach to determine shear capacity of reinforced concrete beams shear strengthened with NSM systems. J Struct Eng 2017;143:4017061. https://doi.org/10.1061/(ASCE)ST.1943-541X.0001793.

[55] ACI Committee 318. Building Code Requirements for Structural Concrete and commentary (ACI 318-14). American Concrete Institute, Farmington Hills, MI, USA.; 2014.

[56] AASHTO. LRFD Bridge Design Specifications. 8th ed. Washington, DC: American Association of State Highway Transportation Officials; 2017.

[57] Japan Society of Civil Engineers. Standard specifications for concrete structures 2007 “Design.” 2007.

[58] CSA Committee A23.3. Design of Concrete Structures (CSA A23.3-14). Can Stand Assoc Mississauga, ON, Canada, 2004, 214 Pp n.d.

[59] Telkamp GJ. Shear Behavior of Reinforced Concrete Beams and Prestressed

Concrete Beams. Itinerario 1981;5:68–9.

[60] Vecchio FJ, Collins MP. The modified compression-field theory for reinforced concrete elements subjected to shear. ACI J Proc 1986;83. https://doi.org/10.14359/10416.

[61] Collins MP, Mitchell D, Adebar P, Vecchio FJ. A general shear design method. ACI Struct J 1996;93:36–45. https://doi.org/10.14359/9838.

[62] Bentz EC, Vecchio FJ, Collins MP. Simplified Compression Field Theory for Calculating Shear Strength of Reinforced Concrete Elements. ACI Struct J 2006;103:614–24. https://doi.org/10.14359/16438.

[63] Lee J-Y, Choi I-J, Kim S-W. Shear behavior of reinforced concrete beams with high-strength stirrups. ACI Struct J 2011;108. https://doi.org/10.14359/51683219.

[64] Cladera A, Marí AR. Shear strength in the new Eurocode 2. A step forward? Struct Concr 2007;8:57–66. https://doi.org/10.1680/stco.2007.8.2.57.

[65] Mansour MY, Dicleli M, Lee JY, Zhang J. Predicting the shear strength of reinforced concrete beams using artificial neural networks. Eng Struct 2004;26:781–99. https://doi.org/10.1016/j.engstruct.2004.01.011.

[66] Abuodeh OR, Abdalla JA, Hawileh RA. Prediction of shear strength and behavior of RC beams strengthened with externally bonded FRP sheets using machine learning techniques. Compos Struct 2020;234:111698. https://doi.org/10.1016/j.compstruct.2019.111698.

[67] Lee S, Lee C. Prediction of shear strength of FRP-reinforced concrete flexural members without stirrups using artificial neural networks. Eng Struct 2014;61:99–112. https://doi.org/10.1016/j.engstruct.2014.01.001.

[68] Chen T, Guestrin C. Xgboost: A scalable tree boosting system. In 22nd SIGKDD

Conference on Knowledge Discovery and Data Mining 2016.

[69] Rahman J, Ahmed KS, Khan NI, Islam K, Mangalathu S. Data-driven shear strength prediction of steel fiber reinforced concrete beams using machine learning approach. Eng Struct 2021;233. https://doi.org/10.1016/j.engstruct.2020.111743.

[70] Feng DC, Wang WJ, Mangalathu S, Hu G, Wu T. Implementing ensemble learning methods to predict the shear strength of RC deep beams with/without web reinforcements. Eng Struct 2021;235. https://doi.org/10.1016/j.engstruct.2021.111979.

[71] Nguyen-Sy T, Wakim J, To QD, Vu MN, Nguyen TD, Nguyen TT. Predicting the compressive strength of concrete from its compositions and age using the extreme gradient boosting method. Constr Build Mater 2020;260. https://doi.org/10.1016/j.conbuildmat.2020.119757.

[72] Nguyen HD, Truong GT, Shin M. Development of extreme gradient boosting model for prediction of punching shear resistance of r/c interior slabs. Eng Struct 2021;235. https://doi.org/10.1016/j.engstruct.2021.112067.

[73] Mangalathu S, Shin H, Choi E, Jeon JS. Explainable machine learning models for punching shear strength estimation of flat slabs without transverse reinforcement. J Build Eng 2021;39. https://doi.org/10.1016/j.jobe.2021.102300.

[74] Machine learning-based prediction of CFST columns using gradient tree boosting algorithm n.d.

[75] Marani A, Nehdi ML. Machine learning prediction of compressive strength for phase change materials integrated cementitious composites. Constr Build Mater 2020;265. https://doi.org/10.1016/j.conbuildmat.2020.120286.

[76] Wong LS, Marani A, Nehdi ML. Gradient Boosting Coupled with Oversampling

Model for Prediction of Concrete Pipe-Joint Infiltration Using Designwise Data Set. J Pipeline Syst Eng Pract 2021;12. https://doi.org/10.1061/(asce)ps.1949-1204.0000557.

[77] Pedregosa F, Varoquaux G, Gramfort A, Michel V, Thirion B, Grisel O, et al. Scikit-learn: Machine Learning in Python. J Mach Learn Res 2011;12:2825–30.

[78] Cortes C, Vapnik V. Support-Vector Networks. Mach Learn 1995;20:273–297. https://doi.org/10.1109/64.163674.

[79] Cherkassky V, Ma Y. Practical selection of SVM parameters and noise estimation for SVM regression. Neural Networks 2004;17:113–26. https://doi.org/10.1016/S0893-6080(03)00169-2.

[80] Sutton CD. Classification and Regression Trees, Bagging, and Boosting. Handb Stat 2005;24:303–29. https://doi.org/10.1016/S0169-7161(04)24011-1.

[81] Freund Y, Schapire RE. A Decision-Theoretic Generalization of On-Line Learning and an Application to Boosting. J Comput Syst Sci 1997;55:119–39. https://doi.org/10.1006/jcss.1997.1504.

[82] Fawagreh K, Gaber MM, Elyan E. Random forests: From early developments to recent advancements. Syst Sci Control Eng 2014;2:602–9. https://doi.org/10.1080/21642583.2014.956265.

[83] Svetnik V, Liaw A, Tong C, Christopher Culberson J, Sheridan RP, Feuston BP. Random Forest: A Classification and Regression Tool for Compound Classification and QSAR Modeling. J Chem Inf Comput Sci 2003;43:1947–58. https://doi.org/10.1021/ci034160g.

[84] Breiman L. Random Forests. Mach Learn 2001;45:5–32.

[85] Segal M, Xiao Y. Multivariate random forests. WIREs DATA Min Knowl Discov

2011;1:80–7. https://doi.org/10.1002/widm.12.

[86] Geurts P, Ernst D, Wehenkel L. Extremely randomized trees. Mach Learn 2006;63:3–42. https://doi.org/10.1007/s10994-006-6226-1.

[87] Mining D. The Elements of Statistical learning - Springer Series in Statistics. Math Intell 2009;27:83–85.

[88] Friedman JH. Greedy Function Approximation: A Gradient Boosting Machine. Ann Stat 2001:1189–232. https://doi.org/10.1214/aos/1013203451.